Journal of Experimental Botany, Vol. 64, No. 8, pp. 2449–2466, 2013
doi:10.1093/jxb/ert106 Advance Access publication 17 April, 2013
This paper is available online free of all access charges (see http://jxb.oxfordjournals.org/open_access.html for further details)

Journal of Experimental Botany
www.jxb.oxfordjournals.org

RESEARCH PAPER

Galacturonosyltransferase 4 silencing alters pectin composition and carbon partitioning in tomato

Fabiana de Godoy[1]*, Luisa Bermúdez[1]*, Bruno Silvestre Lira[1], Amanda Pereira de Souza[1], Paula Elbl[1], Diego Demarco[1], Saleh Alseekh[2], Marina Insani[3], Marcos Buckeridge[1], Juliana Almeida[1], Gabriela Grigioni[4], Alisdair Robert Fernie[2], Fernando Carrari[3] and Magdalena Rossi[1†]

[1] Departamento de Botânica-IB-USP, 277, 05508-900, São Paulo, SP, Brazil
[2] Max Planck Institute for Molecular Plant Physiology, Wissenschaftspark Golm, Am Mühlenberg 1, Potsdam-Golm, D-14 476, Germany
[3] Instituto de Biotecnología, Instituto Nacional de Tecnología Agropecuaría, PO Box 25, B1712WAA Castelar, Argentina
[4] Instituto de Tecnología de Alimentos, Instituto Nacional de Tecnología Agropecuaría, PO Box 25, B1712WAA Castelar, Argentina

* These authors contributed equally to this work.
† To whom correspondence should be addressed. Email: mmrossi@usp.br

Received 7 January 2013; Revised 13 March 2013; Accepted 19 March 2013

Abstract

Pectin is a main component of the plant cell wall and is the most complex family of polysaccharides in nature. Its composition is essential for the normal growth and morphology pattern, as demonstrated by pectin-defective mutant phenotypes. Besides this basic role in plant physiology, in tomato, pectin structure contributes to very important quality traits such as fruit firmness. Sixty-seven different enzymatic activities have been suggested to be required for pectin biosynthesis, but only a few genes have been identified and studied so far. This study characterized the tomato galacturonosyltransferase (GAUT) family and performed a detailed functional study of the *GAUT4* gene. The tomato genome harbours all genes orthologous to those described previously in *Arabidopsis thaliana*, and a transcriptional profile revealed that the *GAUT4* gene was expressed at higher levels in developing organs. *GAUT4*-silenced tomato plants exhibited an increment in vegetative biomass associated with palisade parenchyma enlargement. Silenced fruits showed an altered pectin composition and accumulated less starch along with a reduced amount of pectin, which coincided with an increase in firmness. Moreover, the harvest index was dramatically reduced as a consequence of the reduction in the fruit weight and number. Altogether, these results suggest that, beyond its role in pectin biosynthesis, *GAUT4* interferes with carbon metabolism, partitioning, and allocation. Hence, this cell-wall-related gene seems to be key in determining plant growth and fruit production in tomato.

Key words: fruit metabolism, galacturonic acid, galacturonosyltransferase, pectin, *Solanum pennellii*, tomato.

Introduction

The main role of cell walls is to confer physical strength and provide a barrier against the external environment. Pectins constitute the ~35% of the primary cell wall in eudicot and non-graminaceous monocots, and 2–10% in grasses (Mohnen, 2008). Thus, as a main component of the cell wall, pectins contribute to these two functions together with cellulose and hemicellulose. Pectins include a family of polysaccharides, whose major constituent is galacturonic acid (GalA) (~70%). Four pectin polysaccharides have been described: homogalacturonan (HG), xylogalacturonan

Abbreviations: AIR, alcohol-insoluble residue; Ara, arabinose; Fuc, fucose; GalA, galacturonic acid; GATL, GAUT-like; GAUT, galacturonosyltransferase; GC-MS, Gas chromatography/mass spectrometry; GFP, green fluorescent protein; GX, glucuronoxylan; HG, homogalacturonan; HPAEC/PAD, high performance anion exchange chromatography with pulsed amperometric detection; HPPD, hydroxyphenylpyruvate dioxygenase; qPCR, quantitative PCR; QTL, quantitative trait loci; RG, rhamnogalacturonan; Rha, rhamnose; SGN, Solanaceae Genomics Network; TFA, trifluoracetic acid; XGA, xylogalacturonan; Xyl, xylose; YFP, yellow fluorescent protein.

(XGA), rhamnogalacturonan II (RG-II), and rhamnogalacturonan I (RG-I). HG is a linear polymer made of α-1,4-linked GalA and is the most abundant component of pectin (~65%). XGA is a modified HG with lateral ramifications of xylose attached to the *O*-3 position of some GalA residues. RG-II is a much more complex structure and makes up ~10% of the pectin. In RG-II, the HG backbone is complemented by lateral chains composed of 12 different sugars attached by 22 distinct linkages. Finally, RG-I is the only pectin polysaccharide whose backbone is not exclusively made of GalA but is composed of a disaccharide (α-1,4-D-GalA-α-1,2-L-Rha) repeating unit where the L-rhamnose (Rha) residues may be branched with arabinan, galactan, and/or arabinogalactan (Harholt *et al.*, 2010). Different models have been proposed to explain how these structural elements are combined into a macromolecular structure. The model most consistent with recent results suggests the existence of an RGI-I backbone decorated with side chains composed of the other pectic constituents (Vincken *et al.*, 2003).

Galacturonosyltransferases (GAUTs) are among the enzymes responsible for pectin biosynthesis and belong to a vast group of glycosyltransferases that, together with other carbohydrate active enzymes, are catalogued in the CAZy database (http://www.cazy.org; Cantarel *et al.*, 2009). More specifically, they can be assigned to the glycosyltransferase family 8 (GT8) (Harholt *et al.*, 2010; Yin *et al.*, 2010) consisting of three separate protein classes. class I and class II contain mostly eukaryotic proteins, while class III consists almost entirely of bacterial proteins. The plant cell-wall-related proteins are all located in class I, which includes the galacturonosyltransferase (*GAUT*) genes and the *GAUT*-like (*GATL*) genes (Sterling *et al.*, 2006). An extensive phylogenetic analysis revealed that the GT8 family was acquired from an ancient cyanobacterium progenitor and further separated into subclades, which have undergone functional specialization. Moreover, the increase in the numbers of *GAUT* and *GATL* genes from lower to higher plants suggests that these genes have an important role in plant adaptation to living on land and adopting an upright growth habit (Yin *et al.*, 2010).

In *Arabidopsis thaliana*, 15 GAUT- and 10 GATL-encoding genes have been described, and cumulative evidence indicates that they are involved in cell-wall pectin and hemicellulose biosynthesis (Orfila *et al.*, 2005; Sterling *et al.*, 2006; Caffall *et al.*, 2009; Kong *et al.*, 2011). However, redundancy among the individual GAUTs and pleiotropic effects complicate the assignation of specific functional activities to each protein. Given these problems, only four of them have been functionally characterized to date. Bouton *et al.* (2002) reported that the *A. thaliana* mutant *quasimodo1* (*qua1*), which harbours a T-DNA insertion in the *GAUT8* gene, displays dwarfism and reduced cell adhesion. The *qua1* cell walls contained significantly higher proportions of arabinose (Ara), Rha, and fucose (Fuc), and a lower proportion of uronic acid and xylose (Leboeuf *et al.*, 2005, Orfila *et al.*, 2005). The reduction in cell adhesion in *qua1* was explained by the low content in calcium-dimerized HG, while the alterations of pectin composition indicated modifications of other pectic domains like RG-I side chains (Leboeuf *et al.* 2005). Moreover, Sterling *et al.* (2006) biochemically characterized the homogalacturonan GAUT activity in *A. thaliana*, and identified GAUT1 protein as well as its encoding gene, demonstrating its role in oligogalacturonide elongation. Recently, it has been demonstrated that GAUT1 acts in the Golgi lumen in a complex manner together with GAUT7, which anchors the protein complex to the Golgi membrane (Atmodjo *et al.*, 2011). Finally, the characterization of an *irregular xylem8* (*irx8*) dwarf mutant allowed the proposition that the wild-type locus product, GAUT12, is involved in glucuronoxylan (GX) biosynthesis, a hemicellulosic component of the secondary cell wall in dicot plants. The mutation led to a 57% reduction in the xylose (Xyl) content of GX polysaccharide, and it was proposed that GAUT12 catalyses the addition of an α-D-GalA residue to *O*-4 of the Xyl residue of the β-D-Xyl*p*-(1→4)-β-D-Xyl*p*-(1→3)-α-L-Rha*p*-(1→2)-α-D-Gal*p*A-(1→4)-D-Xyl sequence present at the reducing end of GXs (Peña *et al.*, 2007).

As demonstrated by the characterization of mutant phenotypes, GAUT activity, and consequently pectin composition, is essential for normal growth and morphology (Caffall *et al.*, 2009). Besides this crucial role, in tomato, the amount and composition of pectin and hemicellulose affect fruit firmness (Giovannoni *et al.*, 1989; Tieman *et al.*, 1992; Brummell *et al.*, 1997, 1999*a*,*b*; Saladié *et al.*, 2007; Chapman *et al.*, 2012; Lahaye *et al.*, 2012; Lunn *et al.*, 2013). However, no *GAUT* genes have, as yet, been functionally described in this species. To gain further insight into the function of pectin composition in the whole plant physiology, in this work we characterized the *GAUT* gene family in tomato, focusing on a functional study of a putative GAUT-encoding gene associated with the content of free galacturonate in ripe fruits (Bermúdez *et al.*, 2008). The results demonstrated that this gene affects pectin content and solubility, suggesting that disturbance of cell-wall metabolism causes pleiotropic effects leading to significant changes in growth and carbon partitioning in tomato.

Materials and methods

Plant material, growth conditions, and sampling

Tomato seeds from *Solanum lycopersicum* L. (cv. M82 and Moneymaker) were obtained from the Tomato Genetic Resource Center (http://tgrc.ucdavis.edu). *Nicotiana benthamiana* seeds were obtained from Meyer Beck (Berlin). Tomato and tobacco plants were grown in 20 and 1 litre pots, respectively. The greenhouse conditions were 16 h/8 h photoperiod, 24 ± 3 °C, 60% humidity, and 140 ± 40 μmol m^{-2} s^{-1} incident irradiance.

For expression profile analysis, source (the first totally expanded leaf, which for our cultivar and growing conditions corresponded to the third leaf from the top of the plant) and sink (the first apical leaf not fully expanded) leaves were collected from 8-week-old plants (cv. M82). Fruit pericarps (without placenta and locule walls) at green, mature green, breaker, and ripe stages were harvested 30, 45, 50, and 60 d after anthesis, respectively. All samples were obtained from six independent plants, immediately frozen in liquid N_2, and stored at –80 °C until use. Samples were pooled in three replicates (two independent plants per pool) for further analyses.

For transgenic plant phenotyping, at least three replicates of the selected T0 lines were established. After 16 weeks, source leaves and ripe fruit pericarps were collected as described above. Fruit

biochemical phenotyping was performed exclusively at the ripe stage due to the extremely low fruit production of *GAUT4*-silenced plants. Six-month-old plants were harvested, and fresh and dry aerial biomass were determined. These parameters were used to determine water content and harvest index according to the following formula:

$$\text{Harvest index} = (\text{fruit fresh mass} \times 100)/\text{total aerial biomass}.$$

For heritability assays, 15 T1 plants for each T0 transgenic line were evaluated for the presence of the transgene by PCR. As expected, the transgene segregated at a 3:1 ratio according to a χ^2 test (P <0.05). *GAUT4* expression was reduced by at least 60% for all three transgenic lines (Supplementary Fig. S1A at *JXB* online). In agreement with the T0 phenotype, T1 silenced plants displayed a higher biomass and were taller (Supplementary Fig. S1B; see also Fig. 5A). All measurements in the T1 generation were performed in triplicate in 8-week-old plants.

Light microscopy

Completely expanded leaves were fixed in neutral buffered formalin in phosphate buffer (pH 7.0) for 48 h (Lillie, 1965), dehydrated in a graded ethanol series, and embedded in plastic resin (Historesin Leica; Gerrits, 1991). Cross-sections (10 µm) were cut on a rotating microtome (Reichert Jung Autocut 2040; Leica), stained with 0.05% (v/v) toluidine blue in 0.1 M sodium acetate (pH 4.7) (O'Brien *et al.*, 1964), and analysed with an Olympus BX41 light microscope with a coupled digital camera. Total, palisade, and sponge parenchyma areas were measured using ImageJ software (Rasband, 1997–2012).

Identification and analyses of GAUT sequences

The complete sequence of the *S. lycopersicum GAUT4* gene, Solyc04g015270, was obtained from the Solanaceae Genomics Network (SGN) database (Bombarely *et al.*, 2011). Untranslated regions were determined based on comparison with a reference unigene (U320717) using MULTALIN software (http://www-archbac.u-psud.fr/genomics/multalin.html; Corpet, 1988).

Gene family protein sequences were identified in the SGN database by BLAST search, using the *A. thaliana* and *Oryza sativa* orthologues described by Caffall *et al.* (2009). GAUT protein sequences were aligned using ClustalX (Thompson *et al.*, 1997) and phylogenetic analysis was performed by MEGA5 (Tamura *et al.*, 2011). Evolutionary distances were computed using the JTT matrix-based method (Jones *et al.*, 1992) and expressed as the number of amino acid substitutions per site. The bootstrap values were determined from 1000 trials. As outgroups, an *A. thaliana* (At1g19300; Kong *et al.*, 2011) and *S. lycopersicum* (Solyc02g065530) GATL sequence were included in the analysis. The identified tomato genes were mapped onto the Tomato-EXPEN 2000 genetic map available at the SGN database. The genetic positions were obtained by BLASTN (Altschul *et al.*, 1990) against the entire Tomato-EXPEN 2000 map marker sequence database. Map Chart software 2.2 (Voorrips, 2002) was used to construct the graphical representation of the genetic map. Protein subcellular localization prediction was performed by using TargetP software (Emanuelsson *et al.*, 2007), SherLoc (Shatkay *et al.*, 2007), MultiLoc (Hoeglund *et al.*, 2006), Plant-mPLoc (Chou and Shen, 2010), and iPSORT (Bannai *et al.*, 2002) software. Transmembrane domains were predicted using TMpred (http://www.ch.embnet.org/software/TMPRED_form.html).

RNA isolation and quantitative PCR (qPCR) analyses

Total RNA from 100 mg of samples was extracted with TRIZOL reagent (Invitrogen) according to the manufacturer's instructions. DNA was removed with 1 µl of amplification-grade DNase (Invitrogen) following the recommended protocol. cDNA was synthesized from 1 µg of RNA using random primers and a SuperScript III kit (Invitrogen), and quality was confirmed by PCR using actin intron-flanking specific primers (ActinaUp 5'-TGGCATCATACCTTTTACAA-3' and ActinaLow 5'-TCCGGGCATCTGAACCTCT-3'). Elongation factor 1-α (*EF1-α*), *TIP4*, and *EXPRESSED* were used as housekeeping genes. mRNA levels were quantified by real-time qPCR using a 7500 Real-Time PCR system (Applied Biosystem), SYBR Green Master Mix (Applied Biosystem), and specific primers (Supplementary Table S1 at *JXB* online) at final concentrations of 200 nM. PCR conditions were: 95 ºC for 10 min, 40 cycles of 95 ºC for 15 s, primer annealing temperature for 1 min, and 72 ºC for 30 s. All reactions were performed with two technical replicates and at least three biological replicates.

Data were analysed with LinRegPCR software (Ruijter *et al.*, 2009) to obtain C_t values and primer efficiency. Relative expression and statistics analysis were calculated using fgStatistics software (Di Rienzo, 2009).

Cloning procedures

Primers were designed using the software Oligo Analyzer 3.1 (http://www.idtdna.com) on the basis of unigene sequences. For the GAUT4 subcellular localization experiment, a 699 bp fragment spanning the first 233 aa of the protein was amplified by PCR using Taq Platinum *Pfx* DNA polymerase (Invitrogen) and the following set of primers FUS-GAUT-F (5'-CACCATGAAGATGAAACTGAGGAAGCC-3') and FUS-GAUT-R (5'-TGAACCACCCAATTTGTTG -3'). PCRs were conducted in a total volume of 50 µl containing 0.2 mM of each dNTP, 0.2 mM of each primer, 1× reaction buffer, 1.5 mM $MgClO_4$, 50 ng of cDNA, and 2.0 IU of enzyme. The amplification conditions were: 94 °C for 3 min, 35 cycles of 94 °C for 30 s and 53°C for 30 s, and 68 °C for 3 min. The amplification product was cloned into a pENTR/d-TOPO vector (Invitrogen) and the expression cassette was then transferred to the binary vector pK7FWG2 by recombination using LR clonase (Invitrogen) resulting in a C-terminal green fluorescent protein (GFP) fusion protein (pK7FWG2-GAUTLyc).

For RNAi silencing, a 161 bp fragment of the *GAUT4* gene was used to generate a hairpin construct. The fragment was amplified with the primers GAUTRNAi-F (5'-CACCCGAGCA GCAGTCATACACTAC-3') and GAUTRNAi-R (5'-GTGCAG AGAACACTTCATGAACCAC-3'), and *Taq* DNA polymerase (Invitrogen). The amplicon was cloned into the pENTR/d-TOPO vector (Invitrogen) and transferred into the pK7GWIWG2(I) binary vector using LR clonase, to generate a hairpin construct (pK7GWIWG2(I)-GAUTLyc).

Binary vectors (Karimi *et al.*, 2002) were introduced into *Agrobacterium tumefaciens* strains GV3101 and GV2260 for subcellular localization and plant stable transformation, respectively.

N. benthamiana transient transformation and confocal microscopy

The *Agrobacterium* strains containing pK7FWG2-GAUTLyc, a cytosolic control pK7FWG2-HPPDLyc (full-length cDNA fragment of the hydroxyphenylpyruvate dioxygenase (HPPD) fused to GFP; Almeida *et al.* unpublished results), and a Golgi complex control [based on the cytoplasmic tail and transmembrane domain of GmMan1, soybean α-1,2-mannosidase I fused to yellow fluorescent protein (YFP); Nelson *et al.* 2007] were grown at 28 ºC in LB medium with appropriate antibiotics to an optical density of 0.6 at 600 nm. The cells were harvested, resuspended in 10 mM MES with 100 mM acetosyringone (Sigma), incubated for 4 h in the dark at room temperature, and then infiltrated into leaves of 6-week-old *N. benthamiana* plants. After 48 h, the infiltrated tissues were observed with a confocal laser microscope (Zeiss LSM 400) under a 63× water objective. Chlorophyll images were captured over 590 nm after excitation at 543 nm, while the GAUT:GFP fusion, HPPD:GFP, and Golgi:YFP control were captured over a 505–550 nm range after excitation at 488 nm with an argon laser beam.

Plant transformation

Seedling cotyledons of *S. lycopersicum* (cv. Moneymaker) were used as explants to generate transgenic tomato plants with the hairpin construct pK7GWIWG2(I)-GAUTLyc. *Agrobacterium*-mediated transformation was carried out as described previously (Nunes-Nesi *et al.*, 2005). The presence of the transgene was confirmed by PCR with 35S promoter-specific primers (35S-right, 5'-CCCACTATCCTTCGCAAG-3' and 35S-left, 5'-GCAGGTCACTGGATTTTGG-3'). Thirteen independent T0 transgenic lines were checked for *GAUT4* expression level by qPCR. Three lines were chosen for further detailed phenotypic characterization. *GAUT4* transcript levels were checked in ripe fruits and leaves in at least six biological replicates for each line.

Photosynthetic parameters

Photosynthetic parameters, including gas exchange and chlorophyll fluorescence emission, were evaluated in 4–5-week-old plants, maintained at a fixed irradiance of 140 ± 40 µmol m^{-2} s^{-1} using a Li-Cor 6400 system (http://www.licor.com/), under different light intensities (200, 400, 800, and 1200 µmol m^{-2} s^{-1}), 400 ppm CO_2, and a leaf temperature of 25 ºC. All measurements were performed in dark-adapted plants on the second or third leaflet of the third fully expanded leaf. Photosynthetic parameters were estimated according to the method of Maxwell and Johnson (2000). Non-photochemical quenching (NPQ), photochemical quenching (qP), electron transport rate (ETR), and reduced plastoquinone accumulation (1 – pQ) were estimated using the following equations:

$$NPQ = (Fm - Fm')/Fm'$$

$$qP = (Fm' - Fs)/(Fm' - F0)$$

$$ETR = [(Fm' - Fs)/Fm'] \times fI\alpha leaf$$

$$1 - pQ = (Fs - F0')/(Fm' - F0')$$

where Fm and Fm' are the maximal chlorophyll fluorescence after dark and light adaptation, respectively; Fs is steady-state fluorescence; F0 and F0' are the minimal chlorophyll fluorescence after dark and light adaptation, respectively; *f* is the fraction of absorbed quanta that is used by Photosystem II, which is assumed to be 0.5 for C3 plants; *I* is the incident photon flux density, and αleaf is leaf absorbance, which is assumed to be 0.85 (Sienkiewicz-Porzucek *et al.*, 2010).

Fruit firmness measurements

Firmness was measured on similar-sized intact ripe fruits (60 d after anthesis). Measurements were performed twice on at least one fruit per plant and three plants per line, totalling 44 assessments, according to the method of Smith *et al.* (2002). Each fruit was tested with a cylindrical flat plate (35 mm diameter) with the probe centred over different locules at 90° on the equator of the fruit. Force deformation curves were recorded using a TA.XT Plus Texture Analyzer (Stable Micro Systems) as follows: pre-test speed of 1.5 mm s^{-1}, test speed of 1 mm s^{-1} and a compression distance of 3 mm. Firmness was defined as the maximum at a constant deformation (3 mm).

Soluble sugars and starch quantification

Freeze-dried samples of leaves and fruits were ground in a ball mill (TE 350; Tecnal, Brazil). Ten milligrams of each sample was extracted five times with 1.5 ml of 80% (v/v) ethanol at 80 °C for 20 min. The total extraction volume (7.5 ml) was dried under vacuum and the samples were resuspended in 1 ml of deionized water. To remove pigments, an extraction with 0.5 ml of chloroform was performed. A 500 µl aliquot was used for sugar identification and quantification by high performance anion exchange chromatography with pulsed amperometric detection (HPAEC/PAD) using a Dionex-DX500 system (Dionex, CA, USA) and a CarboPac PA1 column using isocratic elution of NaOH (200 mM). A calibration curve was carried out using standard solutions of glucose, fructose, sucrose, and raffinose with a concentration range from 50 to 200 µM (de Souza *et al.*, 2013). For starch quantification, the pellets obtained after ethanol extraction were washed with water, dried for 1 h at 60°C and incubated for 30 min at 75 °C with 0.5 ml (120 U ml^{-1}) of thermostable α-amylase (EC 3.2.1.1) from *Bacillus licheniformis* (Megazyme, Bray Co. Wicklow, Ireland) in 10 mM MOPS (pH 6.5). This procedure was repeated, giving a total of 120 U of α-amylase. Samples were cooled to 50 °C and then digested with 15 U of amyloglucosidase (EC 3.2.1.3) from *Aspergillus niger* (Megazyme) in 100 mM NaAcO buffer (pH 4.5) twice for 30 min at 50 °C. The enzymatic reaction was stopped by adding 100 µl of 0.8 M percloric acid for protein precipitation. After centrifugation for 5 min at 10 000*g*, an aliquot of 50 µl was incubated with 250 µl of Glucose PAP Liquiform (Centerlab; Brasil) containing glucose oxidase (~11 000 U ml^{-1}), peroxidase (~700 U ml^{-1}), 290 mmol l^{-1} of D-4-aminoantipirine, and 50 mM of phenol (pH 7.5). Using this system,glucose oxidase catalyses glucose oxidation producing H_2O_2 that reacts with D -4-aminoantipirine and phenol under the action of peroxidase. These reactions produce a red antipirilquinonimine whose colour intensity is proportional to the glucose concentration. After 15 min at 30 °C, absorbance was measured on a spectrophotometer coupled to an ELISA reader at 490 nm.

Cell-wall composition

Freeze-dried samples of leaves and fruits (250 mg) were milled for further extraction. After extraction with 80% (v/v) ethanol at 80 °C for five times to remove soluble sugars, 20 ml of 90% (v/v) DMSO was added to the pellets and the suspensions were stirred for 24 h to remove starch, followed by two additions of 20 ml of 90% (v/v) DMSO stirred for 3 h. The supernatants were discarded and the pellets were washed six times with distilled water, freeze dried, and weighed. The remained cell-wall material was termed alcohol-insoluble residue (AIR). AIR was extracted three times in 20 ml of aqueous 0.5% (m/v) ammonium oxalate (pH 7) at 80 °C for 1 h each with stirring. The supernatants (ammonium oxalate-soluble fraction) were combined and dialysed (membrane cut off 12 400) for 12 h against running tap water and then dialysed for 8 h with distilled water, freeze dried, and weighed. To the remaining cell-wall material from leaves, 20 ml of 0.1 M NaOH supplemented with 3 mg ml^{-1} of $NaBH_4$ was added and the suspension was stirred for 1 h. This procedure was repeated twice. The supernatants (NaOH-soluble fraction) were neutralized with glacial acetic acid and dialysed for 12 h with running tap water followed by distilled water for 10 h. The samples were freeze dried and weighed. For both fractions, 2 mg aliquots were hydrolysed by adding 100 µl of 72% H_2SO_4. After 30 min at 30 °C, the solution was diluted to 3% H_2SO_4 and autoclaved for 1 h at 121 °C (Saeman *et al.*, 1945). After deionization through cation- and anion-exchange columns (Dowex), the neutral monosaccharide composition was determined by HPAEC/ PAD in a Dionex DX-500 system using a CarboPac PA1 column. Monosaccharides were eluted in water using a post-column addition of 500 mM NaOH for sugar detection over 40 min and a flow rate of 1 ml min^{-1}.

Uronic acid determination

The amount of uronic acid was quantified in the ammonium oxalate-soluble fraction essentially as described by Filisetti-Cozzi and Carpita (1991). Five milligrams of the freeze-dried material was hydrolysed with 1 ml of H_2SO_4. After 5 min in an ice bath, the procedure was repeated, giving a total of 2 ml of acid. Subsequently, 0.5 ml of water was added and after 5 min on ice, the procedure was repeated. Finally, the mixture was diluted to 10 ml with distilled water. In order to perform the colorimetric assay, 40 µl of 4 M

K-sulfamic acid/potassium sulfamate (pH 1.6) and 2.4 ml of H_2SO_4 containing borate were added to 400 µl of the diluted solution. The mixture was boiled for 20 min. After the addition of 80 µl of 0.15% (m/v) *m*-hydroxybiphenyl in NaOH 0.5% (m/v), the absorbance was read at 525 nm. For each sample, measurements were done in duplicate.

Ascorbic acid

One hundred milligrams of fresh leaf or fruit tissue was extracted with 1 ml of 3% (v/v) trifluoracetic acid (TFA). Five hundred microlitres of the supernatant was applied to an Extract-clean C18 column (500 mg in 8.0 ml, 50 µm average particle size, and 60 Å pore size; Alltech Associates, USA) equilibrated with 100 mM phosphate buffer (pH 7), and column was then eluted with 1.5 ml of 100 mM phosphate buffer (pH 7). To 500 µl of the eluate, 500 µl of 100 mM K_2HPO_4 buffer (pH 8.5) was added. To quantify the total ascorbic acid, 15 µl of 0.1 M dithiothreitol and 125 µl of 3% (v/v) TFA were added to 500 µl of extraction mix. To measure the reduced ascorbic acid, 15 µl of 100 mM phosphate buffer (pH 7) and 125 µl of 3% (v/v) TFA were added to 500 µl of the extraction mix. Both samples were incubated for 3 min at room temperature. Ascorbic acid quantification was performed by HPAEC/PAD using a silica-based reversed-phase C18 column (particle size 5 pm, 150 × 4.6 mm, HL90-5s, Bio-Sil; Bio-Rad, Munich, Germany). The mobile phase consisted of a KH_2PO_4 buffer (100 mM) at pH 3.0 (with phosphoric acid) and was delivered isocratically at a flow rate of 0.5 ml min^{-1}. Ascorbic acid resulted in a peak at 3.5 min. Quantification was done based on standard solutions of reduced and oxidized ascorbic acid.

Gas chromatography/mass spectrometry (GC-MS)

For metabolic profiling, frozen leaves (~100 mg) were extracted in 1.4 ml of methanol, as described by Roessner *et al.* (2001) with the modifications proposed by Lisec *et al.* (2006); 60 µl of internal standard (0.2 mg ml^{-1} of ribitol) was added for quantification. In the case of ripe fruits (~250 mg), the reagent volumes were adjusted using 2 ml of methanol and 120 µl of ribitol, as described by Osorio *et al.* (2012). In both cases, the mixture was extracted for 15 min at 70 °C, mixed vigorously with 1 volume of water, centrifuged at 2200*g*, and subsequently vacuum dried. The residue was redissolved and derivatized for 120 min at 37 °C (in 60 µl of 30 mg ml^{-1} methoxyamine hydrochloride in pyridine), followed by a 30 min treatment at 37 °C with 120 µl of *N*-methyl-*N*-[trimethylsilyl]trifluoroacetamide. Sample volumes of 1 µl were then injected in splitless and split modes, using a hot-needle technique. The GC-MS system was composed of an AS 2000 autosampler, a GC 6890N gas chromatographer (Agilent Technologies, USA), and a Pegasus III time-of-flight mass spectrometer (LECO Instruments, USA). Chromatography was performed with an MDN-35 capillary column of 30 m length, with a 0.32 mm inner diameter and 0.25 µm film thickness (Macherey-Nagel). Samples were injected at 230 °C in splitless mode with helium carrier gas flow set at 2 ml min^{-1}. The flow rate was kept constant with electronic pressure control enabled. The temperature program was isothermal for 2 min at 85 °C, followed by a 15 °C min^{-1} ramp to 300 °C. The transfer line temperature was set at 250 °C. For detection, the temperature of the ion source was set at 250 °C (match transfer line condition). Mass spectra were recorded at 20 scans s^{-1} with a scanning range of 70–660 *m*/*z*. The remaining monitored chromatography time proceeded with the filament turned off. The filament bias current was –70 V and the detector voltage was 1525 V. Both chromatograms and mass spectra were evaluated using ChromaTOF chromatography processing and mass spectral deconvolution software, version 3.00 (LECO Instruments, USA). Identification and quantification were performed with TagFinder 4.0 software and the mass spectra were cross-referenced with those in the Golm Metabolome Database (Kopka *et al.*, 2005; Schauer *et al.*, 2005). Three to six biological replicates were used for this analysis.

Data analyses

Differences in phenotypic parameters were analysed by Infostat software (Di Rienzo *et al.*, 2011). When the data set showed homoscedasticity, an analysis of variance followed by a Tukey or Dunnett test (P <0.05) was used to compare transgenic lines against wild-type controls. Due to lack of homoscedasticity in some cases, a non-parametric comparison was also performed by applying the Kruskal–Wallis test (P <0.05).

Results

GAUT gene family diversity in S. lycopersicum

On the basis of a metabolic quantitative trait loci (QTL) analysis performed in a *Solanum pennellii* introgression line collection (Schauer *et al.*, 2006), we previously identified a putative GAUT-encoding gene co-localizing with a QTL for fruit galacturonate content (Bermúdez *et al.*, 2008). As no *GAUT* genes have been described in tomato and they belong to a large gene family, we first performed a complete phylogenetic analysis. The recently published tomato genome (The Tomato Genome Consortium, 2012) was screened to identify all *GAUT* sequences using *A. thaliana* and *O. sativa* orthologous genes as baits (Caffall *et al.*, 2009). This search retrieved 17 tomato genes. In order to predict the subcellular localization of the encoded tomato proteins, five different programs were tested using At3g61130 (AtGAUT1) and At2g38650 (AtGAUT7) as controls, which have been demonstrated experimentally to localize in the Golgi apparatus (Atmodjo *et al.*, 2011). Interestingly, Sherloc, which predicts using sequence and text-based features (Shatkay *et al.*, 2007), and MultiLoc, which is based on N-terminal targeting sequences (Hoeglund *et al.*, 2006), were those that accurately predicted both proteins to be located within the Golgi. With the exception of SlGAUT2, for which both programs indicated mitochondrial localization, and SlGAUT7, which according to MultiLoc is targeted to the endoplasmic reticulum, all tomato GAUTs seemed to be directed to the Golgi (Table 1).

For each *A. thaliana GAUT* gene, a corresponding tomato orthologue was identified, with the exception of the GAUT12 and GAUT13 clades, which were rather represented by two paralogues in *S. lycopersicum*. The tree topology demonstrated that the GAUT identified by Bermúdez *et al.* (2008) is a GAUT4. The clades for GAUT3, -10, -11, and -15 revealed a single copy in the eudicot and monocot species analysed, and the topology was according to the phylogenetic relationships between them. The GAUT1/2 and GAUT8/9 clades seem to have diverged following the mono/eudicot split, undergoing duplication in the monocot lineage as evidenced by the presence of three rice paralogues. The GAUT4 and GAUT7 clades displayed a single copy in eudicots while being represented by three and five paralogues in rice, respectively. Finally, clades GAUT5/6 and GAUT13/14 exhibited a similar pattern wherein, after the divergence of tomato and *A. thaliana*, gene duplication in the eudicots was followed by a subsequent gene divergence (Fig. 1A). The 17 tomato *GAUT* genes were mapped onto the Tomato-EXPEN 2000 map housed at the SGN website (http://solgenomics.net/) and were found to be evenly distributed among chromosomes 1, 2, 3, 4, 6, 7, 10,

Table 1. Identification of tomato genes encoding for galacturonosyltranferases.

Enzyme[a]	*A. thaliana* locus (no. amino acids)	Tomato unigene[b]	Subcellular localization			Tomato locus[f]	Linked marker[g]	Chromosome position[h] (cM)
			TargetP[c]	SherLoc[d]	MultiLoc[e]			
GAUT1	At3g61130 (673)	SGN-U565384	nd	G	G	Solyc01g093970	P51	1(69 cM)
GAUT2	At2g46480 (528)	SGN-U598345	nd	M	M	Solyc10g017600	T1720	10 (32.5 cM)
GAUT3	At4g38270 (680)	SGN-U567225	SP	G	G	Solyc01g112210	C2_At4g38240	1 (165 cM)
GAUT4	At5g47780 (616)	SGN-U575018	SP	G	G	Solyc04g015270	T0891	4 (53 cM)
GAUT5	At2g30575 (610)	SGN-U574664	SP	G	G	Solyc07g005360	T1112	7 (0.4 cM)
GAUT6	At1g06780 (589)	SGN-U569431	SP	G	G	Solyc12g010200	cLET-8-K4	12 (41 cM)
GAUT7	At2g38650 (619)	SGN-U574191	nd	G	ER	Solyc10g074650	T0283	10 (36 cM)
GAUT8	At3g25140 (559)	SGN-U565194	nd	G	G	Solyc06g083310	U146140	6 (97.2 cM)
GAUT9	At3g02350 (561)	SGN-U563256	M	G	G	Solyc02g089440	cLES-3-G11	2(111 cM)
GAUT10	At2g20810 (466)	SGN-U574750	M	G	G	Solyc04g064490	T0877	4 (67 cM)
GAUT11	At1g18580 (332)	SGN-U565457	M	G	G	Solyc03g114810	cLED-19-N16	3 (107 cM)
GAUT12	At5g54690 (535)	SGN-U601760	nd	G	G	Solyc07g064050	TG438	7 (73 cM)
		SGN-U599179	nd	G	G	Solyc10g006500	T0418	10 (1 cM)
GAUT13	At3g01040 (532)	SGN-U582378	nd	G	G	Solyc02g067060	T0869	2 (21 cM)
		SGN-U563601	nd	G	G	Solyc03g013630	C2_At3g01060	3 (72.7 cM)
GAUT14	At5g15470 (432)	SGN-U573429	nd	G	G	Solyc02g088630	T1480	2(106 cM)
GAUT15	At3g58790 (540)	SGN-U573007	nd	G	G	Solyc07g055930	C2_At3g58790	7 (44.6 cM)

[a] Enzyme name abbreviation.
[b] Tomato unigene number according to SGN (http://solgenomics.net/).
[c] Subcellular localization prediction according to TargetP 1.1 software (http://www.cbs.dtu.dk/services/TargetP/; Emanuelsson *et al.*, 2007). SP, secretory pathway; M, mitochondrion; nd: not determined because output score was below the requested cut-off for localization prediction.
[d] Subcellular localization prediction according to SherLoc (Shatkay *et al.*, 2007). G, Golgi; M, mitochondria.
[e] Subcellular localization prediction according to MultiLoc (Hoeglund *et al.*, 2006). G, Golgi; M, mitochondria; ER, endoplasmic reticulum.
[f] *S. lycopersicum* locus according to SGN (http://solgenomics.net/).
[g] Closest mapped markers.
[h] Chromosome and genetic position in Tomato-EXPEN 2000 v52.

and 12, with no obvious association between genomic localization and phylogenetic distribution (Fig. 1B).

In order to investigate organ expression specificity, a qPCR analysis was performed in leaves and ripe fruits. *GAUT8*, *-12*, *-13*, *-14*, and *-15* showed higher expression in vegetative tissue in comparison with ripe fruits, whereas the rest of the paralogues did not display differential expression between the tested tissues (Fig. 2A). Furthermore, a broader developmental expression profile was carried out for the *GAUT4* gene, which showed it to be ubiquitously expressed. However, increased levels of mRNA were detected in growing tissues such as sink leaves, mature green, and green fruits, although in the latter the increase was not statistically significant (Fig. 2B).

GAUT4 structural characterization

The identification of the genomic clone from *S. lycopersicum* and its comparison with the corresponding mRNA sequence allowed determination of the *GAUT4* gene structure. *GAUT4* was found to be composed of 12 exons with three being non-coding exons. The coding region spanned 2040 nt resulting in a protein of 679 aa (Fig. 3A). The protein topology displayed both transmembrane and GT8 domains. Within the latter, the characteristic GT8 motif DxD was present. Moreover, the GAUT family-specific motif described previously by Sterling *et al.* (2006) was also identified, albeit showing an amino acid substitution with respect to the *Arabidopsis*/rice consensus sequences. *In silico* analysis of the protein primary structure suggested that GAUT4 is targeted to the Golgi (Table 1) and probably remains anchored to the membrane, as evidenced by the presence of a transmembrane domain (Fig. 3B). This result is in agreement with the localization of the GAUT4:GFP fusion protein for which the punctate fluorescence signal in the cytoplasm of mesophyll cells matched that which would be anticipated for proteins targeted to this subcellular compartment (Fig. 3C).

Generation and primary characterization of GAUT4-silenced plants

With the aim of gaining further knowledge about GAUT4-specific function, *S. lycopersicum* transgenic lines expressing a *GAUT4* hairpin construct were generated. The level of silencing was assessed by qPCR in source leaves and ripe fruits, and three lines showing significantly reduced levels of *GAUT4* mRNA (RNAi2, RNAi40, and RNAi42) were propagated for further phenotypic characterization (Fig. 4). As functional redundancy has been hypothesized within the GT family (Mohnen, 2008), the expression levels of the other four uncharacterized *GAUT* genes (*GAUT3*, *-7*, *-10*, and *-15*) were investigated in the leaves and fruits of the transgenic lines. These genes were chosen because they belong to different clades of the *GAUT* phylogeny spanning all the gene family diversity. Neither co-silencing effects nor compensatory upregulation were detected for any of the tested genes (data not shown).

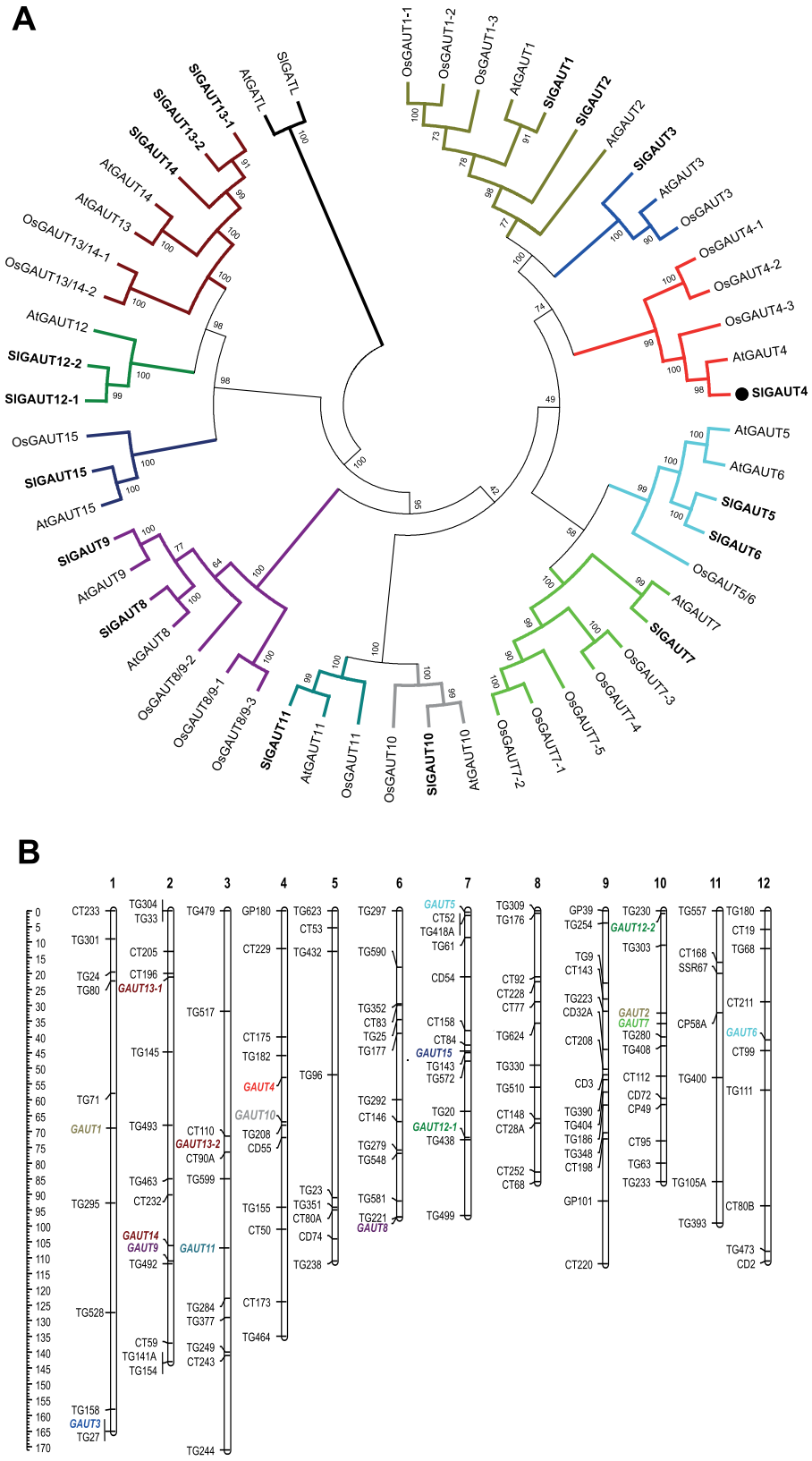

Fig. 1. The GAUT protein family and genomic localization of *GAUT* genes in tomato. (A) Phylogenetic analysis of the GAUT family in *A. thaliana* (At), *O. sativa* (Os), and *S. lycopersicum* (Sl). *A. thaliana* and *O. sativa* sequences were obtained from Caffall *et al.* (2009). The tomato orthologues were identified in this work. The tree was rooted with AtGATL and SlGATL, which are GATL proteins from *A. thaliana* and *S. lycopersicum*, respectively. Bootstrap values greater than 50% are indicated on the branches. The black dot identifies the gene described by Bermúdez *et al.* (2008). (B) The 17 identified genes were localized in the Tomato-EXPEN 2000 genetic map available at the Solanaceae Genomics Network (http://solgenomics.net/index.pl). Markers and *GAUT* genes are indicated on the left side of the chromosomes. *GAUT* genes are highlighted in the same colour pattern as their branches on the phylogenetic tree. Genetic distances are indicated on the left border.

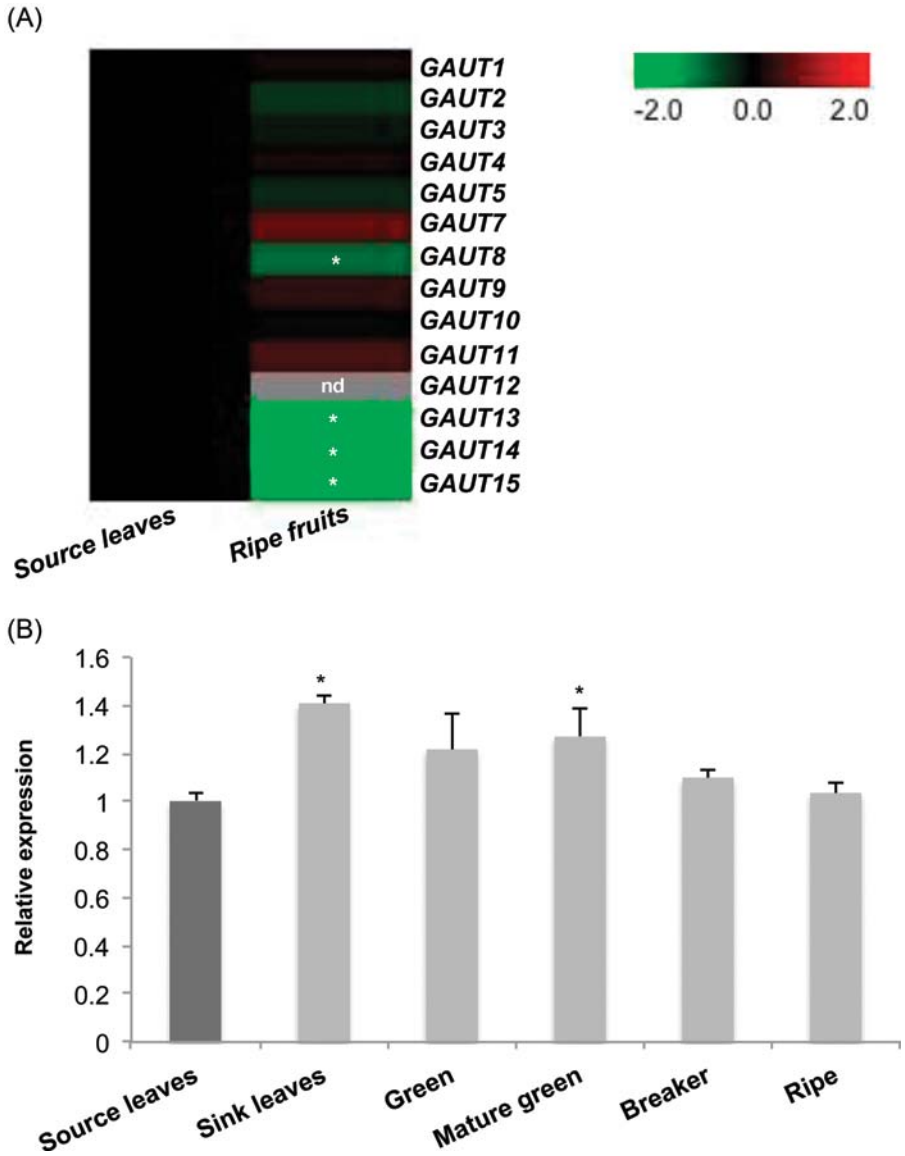

Fig. 2. Expression profiles of *GAUT* genes in tomato. (A) Gene expression profiles of 14 members of the *GAUT* gene family were measured by qPCR in samples from source leaves and ripe fruits (n=3). Relative gene expression levels (log_2) are shown using a colour scale where green and red indicate decreased and increased transcript levels in ripe fruits with respect to source leaves (black boxes), respectively. Grey boxes indicate that the gene was not detected (nd). The heat map was constructed using MeV software (Saeed *et al.*, 2003). *GAUT12* and *GAUT13* represent the expression of both paralogue pairs: *GAUT12-1* and *GAUT12-2*, and *GAUT13-1*, and *GAUT13-2*. (B) *GAUT4* gene expression profile in source and sink leaves, and in green, mature green, breaker, and ripe fruits. The data indicate relative expression normalized to source leaf value (black bar). All data are means from at least three biological replicates. Significant statistic differences from source leaves are indicated: *P <0.05.

Carbon assimilation and other photosynthetic parameters were evaluated at the vegetative stage of the plants and no significant differences were observed between silenced and control plants (Supplementary Table S2 at *JXB* online). Despite these results, *GAUT4*-silenced plants showed higher levels of vegetative growth, as revealed by the size of 8-week-old T1 plants (Fig. 5A and Supplementary Fig. S1). The biomass increment (Fig. 5B) was mainly due to an increase in the leaf water content, which increased ~4% in the silenced plants (Fig. 5D). To gain insights about the origin of the biomass increment, morphometric analyses were performed from source leaf cross-sections of the T1 plants. The palisade parenchyma was larger in transgenic plants compared with wild-type controls (Supplementary Fig. S2A, B). Furthermore, the cell density was also higher in this tissue (Supplementary Fig. S2C) in accordance with the differences in growth parameters.

On assessing fruit characteristics, while flowering time was unaltered, the number (Fig. 5E) and weight (Fig. 5F) of fruits, as well as the harvest index (Fig. 5G) decreased significantly in the transgenic plants. However, transgenic ripe fruits were more resistant to pressure, as demonstrated by the flat plate compression test (Fig. 5H). Due to insufficient fruit

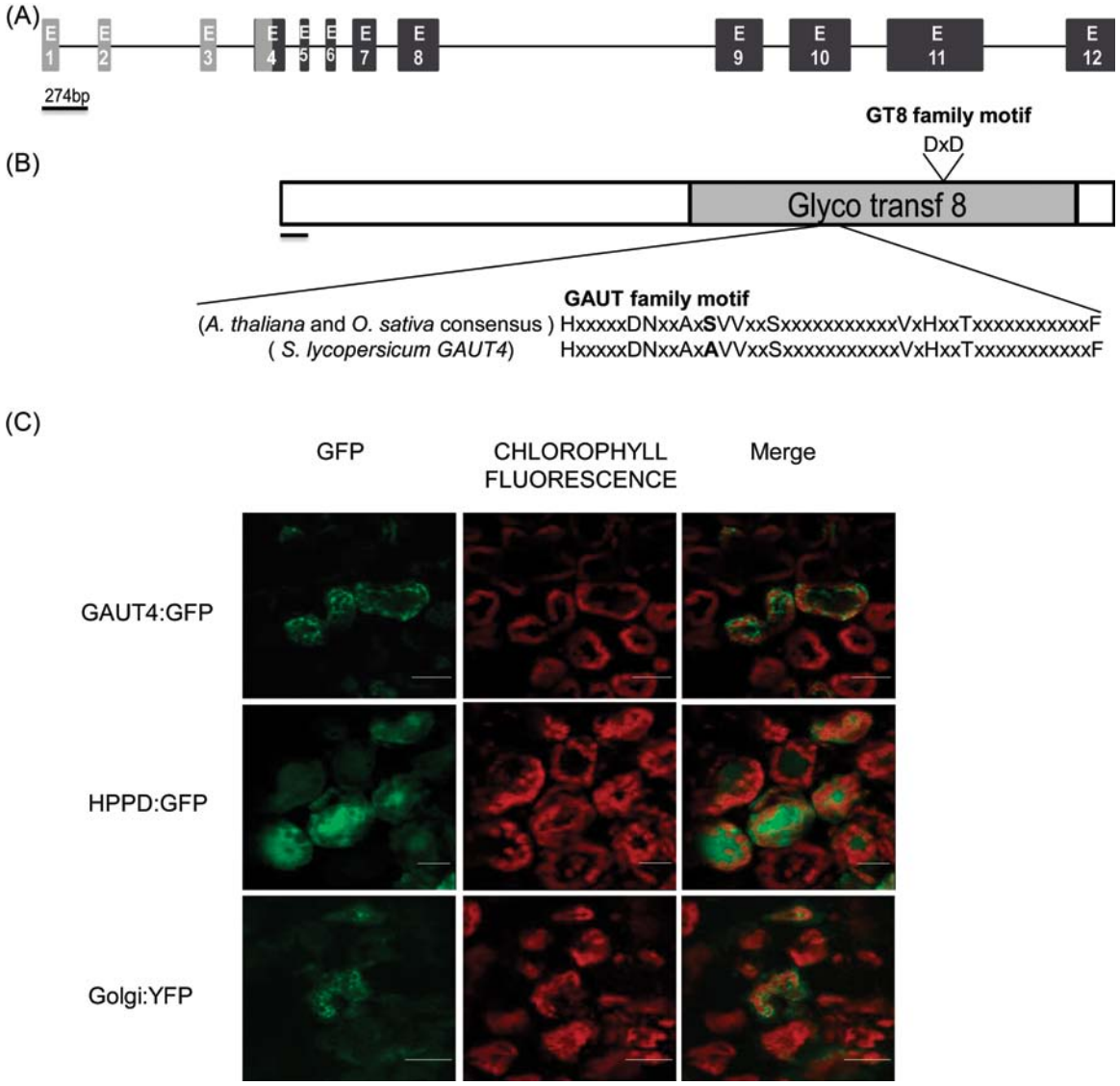

Fig. 3. Structure of the tomato *GAUT4* gene and protein localization. (A) Structure of the tomato *GAUT4* gene. Exons are indicated as E. Coding and non-coding exons are in black and grey, respectively. Lines represent introns. (B) Schematic representation of the GAUT4 protein structure exhibiting the GT8 domain (Glyco_transf 8) as a grey box with the family characteristic motifs, GT8 and GAUT. The dark line indicates the position of the transmembrane domain. (C) Confocal imaging of *N. benthamiana* mesophyll cells expressing GAUT4:GFP, HPPD:GFP (a cytosolic control), and Golgi:YFP (a Golgi complex control) fusion proteins. GFP, chlorophyll fluorescence, and merged signals are indicated above the panels. Bars, 25 μm for GAUT4:GFP and HPPD:GFP fusions; 50 μm for Golgi:YFP control.

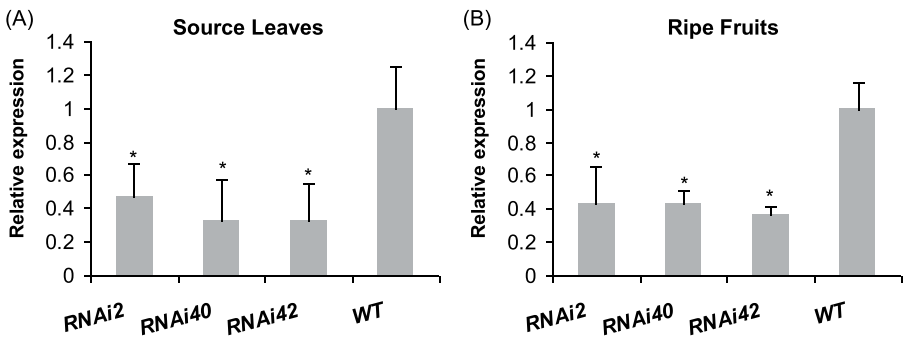

Fig. 4. *GAUT4* expression levels in silenced transgenic plants. *GAUT4* expression was measured by qPCR in samples from source leaves (A) and ripe fruits (B). Data indicate relative expression means from at least three biological replicates normalized to the wild-type (WT) value. Significant statistic differences from the wild type are indicated: *P <0.05.

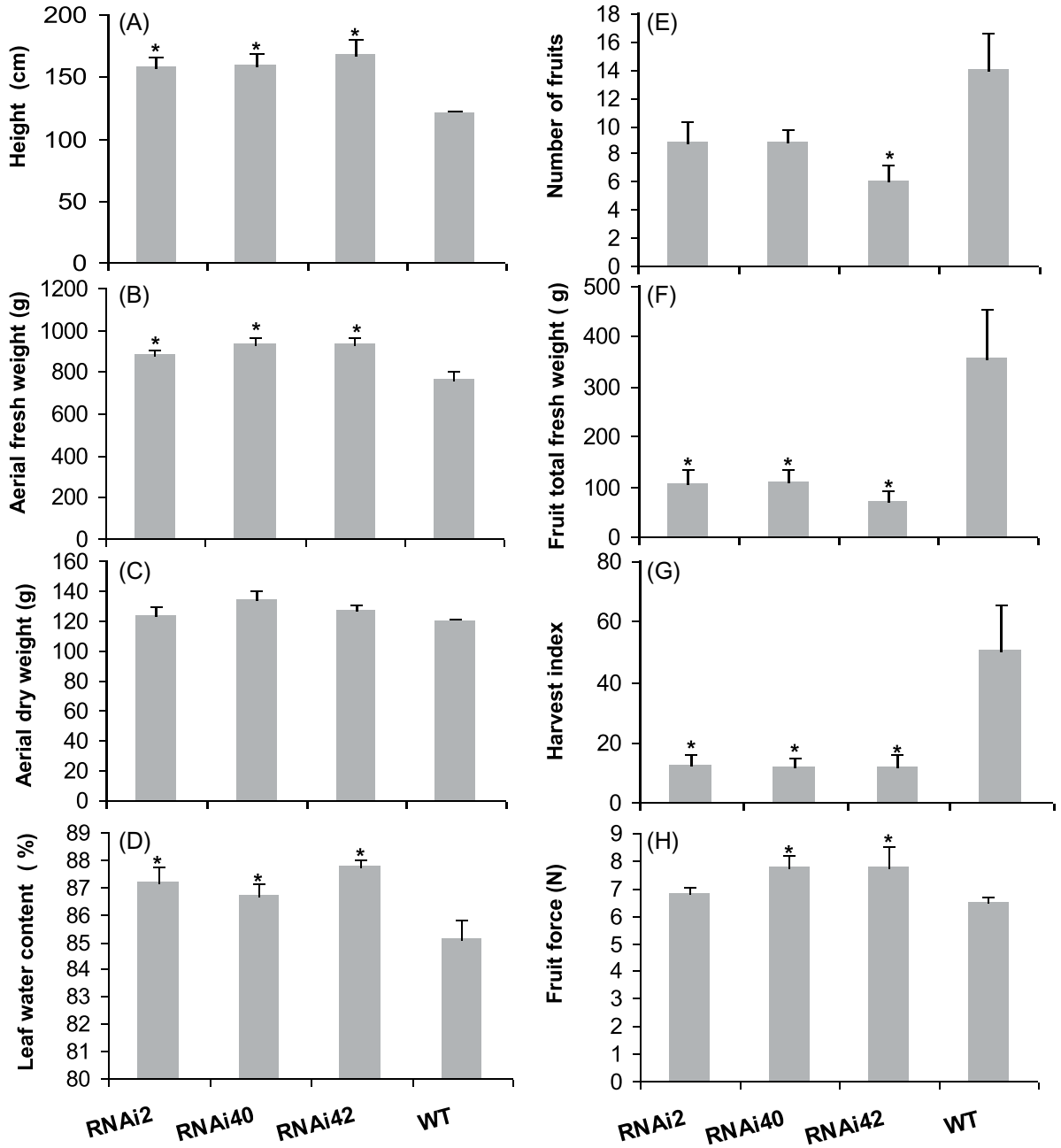

Fig. 5. Phenotypic characterization of the *GAUT4*-silenced plants. (A) Height of wild-type (WT) and T1 silenced plants at 8 weeks old from the base to the apex. (B–D) Six-month-old T0 plants were harvested and fresh (B) and dry (C) aerial biomass, and leaf water content (D) were calculated. (E–G) For fruits, the total number of fruits (E) and total fruit weight (F) at harvest time were measured, and the harvest index (G) was calculated. (H) Firmness was measured for intact fruits at the ripe stage. Values are means from at least three biological replicates for (A)–(G), and from at least five fruits per line for (H). Significant statistic differences from the wild type are indicated: *P <0.05.

production of *GAUT4*-silenced plants, further biochemical characterization was performed exclusively at the ripe stage, impeding evaluation across fruit development.

Biochemical characterization of GAUT4-silenced plants

As *GAUT4* was expected to be involved in pectin synthesis, a cell-wall fractionation was performed in order to evaluate the impact of this gene silencing on the cell-wall composition. From leaf tissue, two cell-wall fractions were evaluated in which all pectic polysaccharides were supposedly extracted: the chelator-soluble fraction, extracted with ammonium oxalate; and the alkali-soluble fraction, extracted with 0.1 M NaOH. In the latter, hemicellulose traces could also be present. After the ammonium oxalate extraction, an unworkable amount of material remained from fruit pericarp, and thus only the chelator fraction was assessed for this tissue. In leaves of silenced plants, the cell wall was basically unaltered,

both in amount (Fig. 6) and composition (Table 2). By contrast, transgenic fruits contained less ammonium oxalate-soluble pectin (Fig. 6) with reduced content of Rha, Ara, and galactose (Gal) (Table 2). For interpretation of the occurrence and properties of cell-wall polysaccharides from sugar composition, three sugar ratios were analysed: a measure for the linearity of pectin, the contribution of RG-I to the entire pectin population, and the extent of branching of RG-I (Houben *et al.*, 2011). The ratios suggested that *GAUT4* silencing affects RG-I accumulation, specially based on Rha/uronic acids ratio, with a clear stronger impact on fruits. Interestingly, in both analysed organs, RG-I branching in transgenic plants was increased by 26% (Table 3).

To identify whether the reduction in *GAUT4* expression could be associated with a shift of plant metabolism in general, a detailed evaluation of primary metabolism was carried out by GC–MS and HPLC. The resultant metabolic profile showed that *GAUT4* silencing did not produce massive biochemical changes but rather only specific alterations in a handful of metabolites (Supplementary Table S3 at *JXB* online). It is worth noting that free GalA was slightly increased in leaves, while the increment was more significant in fruits in agreement with the lower pectin amount observed in the latter organ (Fig. 7A, B). Raffinose was the only altered soluble sugar displaying consistently decreased levels in the leaves of the transgenic plants (Fig. 7C).

Finally, in an aim to understand better the relationship between the increase in vegetative biomass and the strong reduction in harvest index, the starch contents were enzymatically quantified. Whereas in leaves no significant changes were observed, in fruits the accumulation of this polymer was reduced, suggesting a shift in carbon partitioning between source and sink tissues (Fig. 8).

Discussion

GAUT genes encode a set of enzymes belonging to the CAZy GT8 family of glycosyltransferases that are associated with pectin and hemicellulose biosynthesis (Cantarel *et al.*, 2009). In the present study, we performed genomic identification of the *GAUT* gene family in *S. lycopersicum* and functional characterization of the *GAUT4* member. After the identification of all *GAUT* genes encoded in the tomato genome, the phylogenetic analysis revealed that the tomato genome harbours all the genes orthologous to those previously described for *A. thaliana*. Caffall *et al.* (2009) reported the existence of two copies of *GAUT12* in poplar, while no orthologues were identified in rice. In tomato, our survey retrieved also two *GAUT12* genes, re-enforcing the hypothesis that GAUT12 has a specialized role in the synthesis of secondary wall GX of dicot walls, as proposed by Persson *et al.* (2007). The tree topology also suggested that *GAUT12* constitutes a monophyletic group with *GAUT13* and *GAUT14*. This finding is in discrepancy with the phylogeny proposed by Caffall *et al.* (2009), in which *GAUT15* appeared more closely related to the *GAUT13/14* clade. Three pairs of recently duplicated genes that originated after the split between *A. thaliana* and *S. lycopersicum* were identified: *SlGAUT5* and *SlGAUT6*, and *SlGAUT12-1* and *SlGAUT12-2*, as well as *SlGAUT13-1* and *SlGAUT13-2* and *SlGAUT14*. The 17 tomato *GAUTs* were mapped, and interestingly those pairs of genes that were closely linked according to the phylogenetic analysis were distantly located within the

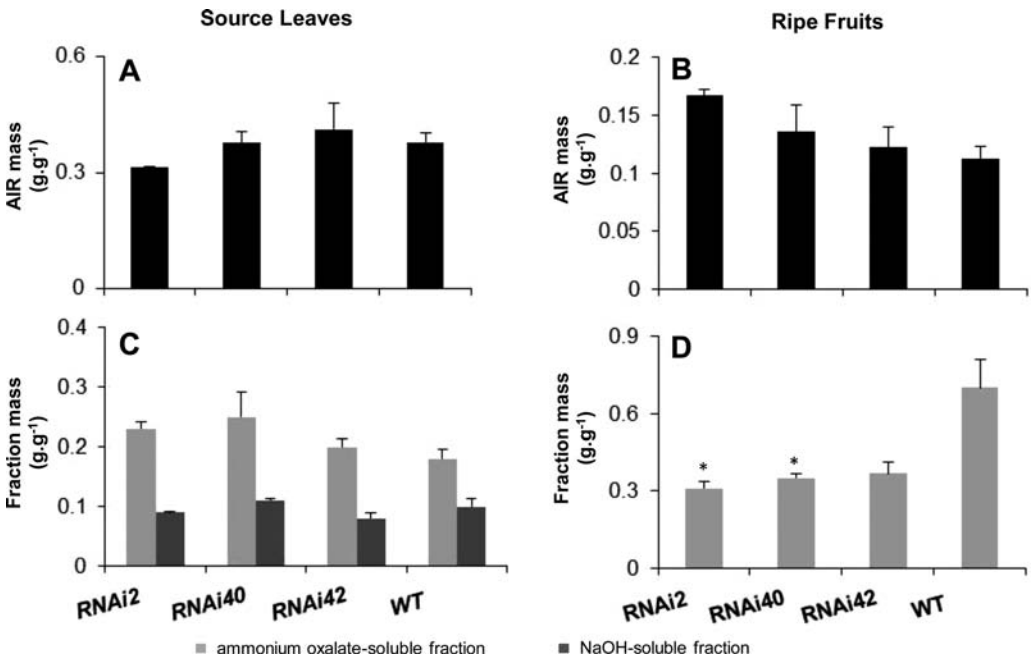

Fig. 6. Cell-wall polysaccharide content in *GAUT4*-silenced plants. (A, B) The alcohol-insoluble fraction (AIR) containing the cell wall was extracted from leaves (A) and fruits (B) and expressed relative to dry material. (C, D) AIR was fractioned by subsequent extractions with ammonium oxalate and NaOH from source leaves (C) and only with ammonium oxalate from ripe fruits (D). The mass for each fraction was expressed relative to AIR. Significant statistic differences from the wild type for any given fraction are indicated: *$P<0.05$.

Table 2. Sugar composition of the cell-wall fractions of transgenic lines.

		Sugar content in ammonium oxalate-soluble fraction (μg g^{-1} AIR)					Sugar content in NaOH-soluble fraction (μg g^{-1} AIR)				
		Fucose[a]	Rhamnose[a]	Arabinose[a]	Galactose[a]	Xylose[a]	Uronic acids[b]	Fucose[a]	Rhamnose[a]	Arabinose[a]	Galactose[a]	Xylose[a]
Leaves	RNAi2	23.4±1.3	274.4±65.9	403.8±54.7	326.9±115.1	36.6±3.1	102,153.9±10,424.2	5.1±0.4	24.6±6.5	209.3±8.9	136.1±24.8	44.2±15.5
	RNAi40	22.0±6.8	288.7±81.9	493.0±178.8	399.2±144.8	27.8±6.6	107,127.6±8,695.0	5.5±0.5	32.9±6.1	211.0±14.7	310.0±25.6	38.0±2.6
	RNAi42	22.3±1.3	237.3±40.6	460.4±21.3	372.8±17.2	31.0±6.8	104,676.3±16,229.8	4.4±0.6	35.2±15.6	220.9±54.9	282.4±107.5	26.6±3.4
	WT	24.1±4.1	314.6±55.3	397.4±52.3	321.8±42.4	41.8±3.1	100,326.8±8,536.2	4.7±0.7	27.6±6.4	182.4±29.9	135.6±16.3	33.3±5.8
Fruits	RNAi2	79.2±18.9	**100.7±13.5**	**609.8±73.0**	1,618.5±168.4	237.7±48.8	140,641.2±4,141.9					
	RNAi40	114.2±24.6	**73.7±16.7**	**436.4±81.6**	**983.1±196.0**	196.2±53.2	168,608.4±34,643.9					
	RNAi42	88.1±24.6	152.4±20.9	669.7±36.9	**1527.1±163.2**	196.6±12.0	201,196.4±11,135.3					
	WT	171.7±35.3	353.5±81.6	1,417.5±141.2	3424.6±135.5	739.5±29.1	192,813.6±564.6					

[a] Monosaccharaides were measured by HPAEC/ PAD in ammonium oxalate and NaOH-soluble fractions.

[b] Uronic acids were quantified spectophotometrically in the ammonium oxalate-soluble fraction. Data indicate means from at least three biological replicates. Significant statistic differences from the wild type (WT) are indicated in bold (P <0.05).

genome, suggesting that they have arisen from a segmental duplication followed by a genomic rearrangement of the tomato genome (Song *et al.*, 2012). A similar observation has also been reported for tomato tocopherol biosynthetic genes (Almeida *et al.*, 2011). Moreover, Kong *et al.* (2011) determined the relationship between *GATL* paralogous genes also based on the segmental duplication history of the corresponding genomic regions in *A. thaliana* (Blanc and Wolfe, 2004).

Expression profiles suggested that, although cell-wall biosynthesis/degradation is a ubiquitous metabolic process in plant cells, there is a certain degree of organ/tissue specificity in GAUT activity probably associated with differential pectin composition. Tissue specificity has previously been demonstrated for *GAUT* genes. In this sense, by using *in situ* PCR, Orfila *et al.* (2005) demonstrated that *GAUT8* from *A. thaliana* is expressed in discrete regions around the vascular bundles. Similarly, *GAUT12* was also expressed in vascular tissues in *A. thaliana*, as revealed by promoter:*gus* fusion studies (Persson *et al.*, 2007). In tomato, *GAUT8* and *GAUT12* are more highly expressed in leaves than in fruits. As vascular tissue density is much more abundant in leaves than in the fruit pericarps, our results suggest a similar expression pattern to that shown for the *A. thaliana* orthologous loci. Interestingly, *GAUT13*, *GAUT14*, and *GAUT15*, which cluster together with *GAUT12*, had a similar expression pattern, possibly indicating similar function as proposed by Caffall *et al.* (2009). In particular, *GAUT4* was expressed ubiquitously, as was also observed in *A. thaliana*. However, higher expression levels were documented in growing stages, pinpointing its crucial role in normal development, as indicated by the lack of ability to rescue the corresponding *A. thaliana* mutant (Caffall *et al.*, 2009).

Pectic polysaccharides are synthesized in the Golgi apparatus of plant cells, sorted to vesicular compartments, and subsequently secreted to the apoplastic space (Caffall and Mohnen, 2009). Phylogenetic analysis, structural characterization, and subcellular localization experiments demonstrated that the gene under study is indeed the tomato *GAUT4* gene. Moreover, the results are in close agreement with the assumed model for biosynthesis of pectin/hemicellulose cell-wall polymers in which enzyme active sites face the Golgi lumen, being anchored, directly or indirectly, by transmembrane domains (Peña *et al.*, 2007; Caffall and Mohnen, 2009; Atmodjo *et al.*, 2011).

Pectin comprises as much as 30% of dicot cell walls (Ridley *et al.*, 2001). Two-thirds of the worldwide tomato production concerns processing tomato, with modifications in the structure and composition of pectin being directly related to alterations in juice texture and extractability (Sila *et al.*, 2009). Moreover, intact fresh fruit texture is a quality index for consumption *in natura* (Barrett *et al.*, 1998; Lahaye *et al.*, 2012). To gain further insights about pectin metabolism and particularly the role of the *GAUT4* gene, tomato transgenic plants expressing a hairpin RNA construct were obtained. The ripe fruits of silenced lines displayed significantly lower levels of ammonium oxalate-soluble pectin and the pectin contained reduced contents of Rha, Gal, and Ara. These data, together with the reduction of 70%

Table 3. Sugar ratios for the different polysaccharide fractions of transgenic lines. Ratios were calculated based on Table 2 data.

		Linearity of pectin	Contribution of RG-I to pectin population	Branching of RG-I
		Uronic acids/ (Xyl+Gal+Rha+Ara+Fuc)	Rha/uronic acids	(Ara+Gal)/Rha
Leaves	RNAi plants	91.2	0.0026	3.1
	WT plants	91.2	0.0031	2.3
Fruits	RNAi plants	74.3	0.0006	18.6
	WT plants	28.5	0.0020	13.7

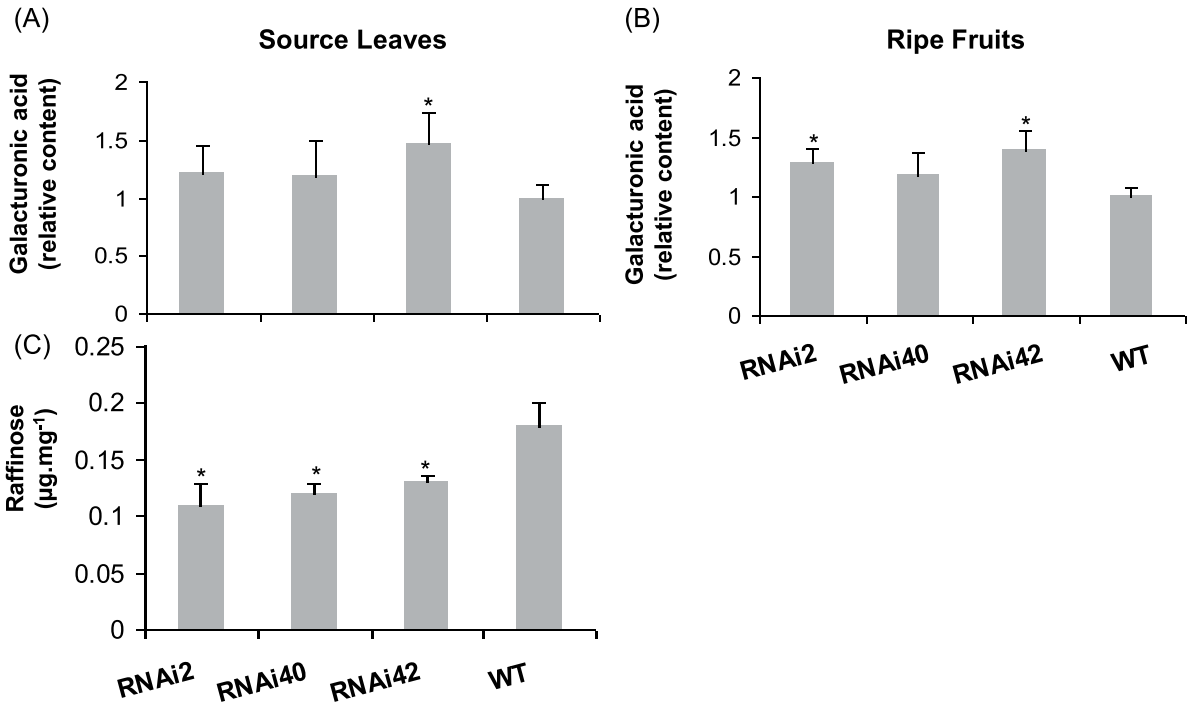

Fig. 7. Soluble metabolite content in *GAUT4*-silenced plants. (A, B) GalA was quantified by GC-MS from source leaves (A) and ripe fruits (B) and data were normalized to wild type (WT) and expressed as relative content. (C) Free raffinose content in source leaves was measured by HPLC and expressed relative to dry weight. This monosaccharide was not detected in ripe fruits in agreement with the decrease across fruit development reported by Oms-Oliu *et al.* (2011). All values indicate means from at least three biological replicates and significant statistic differences from the wild type are indicated: *$P<0.05$.

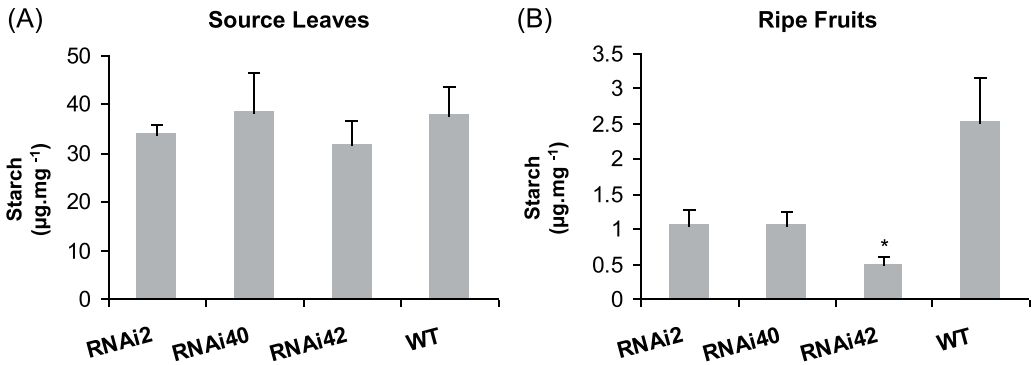

Fig. 8. Starch content in *GAUT4*-silenced plants. Starch was quantified enzymatically in source leaves (A) and ripe fruits (B). Values are expressed relative to dry weight. Data indicate means from at least three biological replicates. Significant statistic differences from the wild type are indicated: *$P<0.05$.

in Rha/uronic acids ratio, suggest that GAUT4 plays a role in RG-I backbone synthesis. The absence of the observed effect in leaves could be explained by the compensation of other paralogues that are also expressed in leaves but not in fruits *(i.e. GAUT2*, *-5*, *-13*, *-14*, or *-15*). These other enzymes could either have a similar biochemical function and/or culd balancing the lack of RG-I producing other polymers or altering branching pattern, leading to slight alterations in sugar ratios. In this sense, in both analysed organs, an increased level (26%) of RG-I branching was observed. Transgenic potato plants with a reduced proportion of RG-I displayed an increase in uronic acid content also exposing pectin biosynthesis compensation (Oomen *et al.*, 2002).

In contrast to previous reports on GAUT-deficient plants, which displayed dwarfism (Bouton *et al.* 2002; Peña *et al.* 2007; Persson *et al.* 2007), *GAUT4* silencing resulted in taller plants with higher vegetative biomass. The morpho-anatomical analysis of the leaves highlighted the increased water content and fresh mass observed in transgenic plants. The reduction in GAUT4 activity might have resulted in a looser cell wall; thus, in order to keep the pressure potential and consequently the water potential constant, the compact palisade parenchyma became enlarged and increased the cell density. This is in line with evidence indicating that hydraulics play an essential but passive role in controlling cell growth (Szymanski and Cosgrove, 2009; Alim *et al.*, 2012).

Intriguingly, the silencing of *GAUT4* resulted in a decreased provision of carbon to sink tissues. This was evidenced by the decreased harvest index, mostly as a consequence of the reduction in total fruit weight and number associated with a lower fruit starch accumulation. Recently, Wormit *et al.* (2012) demonstrated that carbohydrate metabolism is responsive to changes in cellulose biosynthesis via an osmosensitive mechanism. All phenotypic data presented here including growth parameters, biochemical profile, and histological analyses suggested that the pleiotropic effects caused by *GAUT4* silencing are the consequence of the same metabolic crosstalk, and they allow extension of the proposed mechanism to cell-wall biosynthesis.

Regarding this unknown metabolic crosstalk, our data provide evidence supporting the hypothesis that raffinose represents an important carbon source during fruit set and early development (Patrick and Offler, 1996; Nguyen-Quoc and Foyer, 2001), as its level was reduced in the source leaves of the transgenic plants. Raffinose is synthesized from UDP-Glc by subsequent reactions catalysed by UDP-glucose 4-epimerase (EC 5.1.3.2), galactinol synthase (EC 2.4.1.123), and raffinose synthase (EC 2.4.1.82). The latter combines galactinol and sucrose to produce *myo*-inositol and raffinose (Unda *et al.*, 2012). In this regard, it has been demonstrated that, despite strong evidence for apoplastic unloading of sugars (Fridman *et al.*, 2004; Hackel *et al.*, 2006), a functional symplastic continuity of cell connections and numerous plasmodesmata between the phloem and storage parenchyma cells exists in young fruits. It is thus conceivable that carbon is partially unloaded via the symplast and, therefore, raffinose might represent an important carbon source. Virtually, all cell-wall precursors are derived from UDP-D-glucose (UDP-Glc) and GDP-D-mannose (GDP-Man) nucleotide sugars via a series of mechanistically related reactions that are cataysed by 4-epimerases, 3,5-epimerases, 4-reductases, 4,6-dehydratases, dehydrogenases, and decarboxylases (Reiter, 2008). Thus, the reduction of GAUT4 activity could unbalance nucleotide sugar interconversion reactions leading to a raffinose content reduction in transgenic lines once it is synthesized from UDP-Glc (Caffall and Mohnen, 2009). Moreover, the sucrose reduction trend observed in leaves of silenced plants re-enforces this hypothesis.

Fruits of transgenic plants exhibited increased firmness. During tomato ripening, a decrease in the hydrostatic pressure (turgor) within fruit cells has been well documented to contribute to softening (Shackel *et al.*, 1991). Presumably, this is due to a combination of events that lead to a dilution of the cell content and/or the direct loss of water from the fruit. These events may include: redistribution of solutes or solute leakage from the cell, breakdown of cell-wall structure, and transpiration. The elevation in apoplastic solute concentrations may occur as a result of increasing membrane leakiness and/or breakdown of complex cell-wall polysaccharides into smaller soluble components (Harker *et al.*, 1997). Although membrane structure remains intact during fruit ripening, membrane conductivity (permeability) increases and thus there is a tendency for solutes to leak into the extracellular fluid, for the cell wall to hydrate, and for intercellular spaces to become water-soaked (Harker *et al.*, 1997). However, the possible influence of solutes derived from cell-wall catabolism on the osmotic potential of the apoplast fluid has not been demonstrated. In this context, the higher firmness found in *GAUT4*-silenced fruits could be explained by the following hypotheses. First, as a lower amount of ammonium oxalate-soluble pectin was observed, less intercellular solute accumulation might explain the higher cell turgor. Recently, Lunn *et al.* (2013) reported a similar phenotype where transgenic tomatoes with a blockage in pectin deposition showed a reduced amount of pectin together with an increase in fruit firmness. Secondly, the reduction in carbon influx observed in transgenic fruits could alter the increase in membrane conductivity, while the increment in free GalA contributes to water retention. Further experiments will be conducted to clarify the mechanisms underlying this phenomenon.

Our results additionally bring insights to explain the impossibility of identifying *gaut4* mutants in *A. thaliana*, described by Caffall *et al.* (2009). First, it has been reported that *A. thaliana* seed mucilage is primarily composed of RG-I (Arsovski *et al.*, 2009); hence, a *gaut4* mutation would compromise seed viability. Secondly, raffinose is an important source of carbon storage and desiccation tolerance in *Arabidopsis* seeds and consequently the alteration of nucleotide sugar interconversion reactions would compromise UDP-Glc production and ultimately raffinose biosynthesis (Zhou *et al.*, 2011).

Interestingly, *GAUT4*-silenced plants mimic the *S. pennellii* introgressed line 4-3-2 (IL4-3-2). This line exhibited a lower amount of *GAUT4* mRNA (Fei *et al.*, 2011), showed a fruit free GalA QTL, and exhibited dramatically reduced yield (Schauer *et al.*, 2006). Likewise, the transgenic plants analysed here displayed less pectin and an increase in free GalA in the

fruits, as well as a reduction in the harvest index. Therefore, the results shown in this work suggest that the *GAUT4* gene is one of, or the sole, genetic determinant(s) of the *S. pennellii* introgressed line phenotype as we suggested previously (Bermúdez *et al.* 2008). In the same genomic region of chromosome 4, Chaïb *et al.* (2006) mapped a QTL for fruit mealiness and instrumental firmness. Furthermore, biochemical characterization revealed alterations in pectin composition as well as in cell size (Lahaye *et al.*, 2012, 2013), in agreement with the results presented here.

In conclusion, our results have presented characterization of the *GAUT* gene family in tomato and showed that changes in the structure of cell-wall polysaccharides correlate with their spatial and temporal locations in developing plant tissues. Moreover, silencing of the *GAUT4* gene altered pectin composition and affected plant growth and development. The observed phenotypes revealed physiological mechanisms, via cell-wall polysaccharides and raffinose metabolisms, that modulate plant resource allocation, resulting in an unprecedented shift in source to sink carbon partioning in tomato.

Supplementary data

Supplementary data are available at *JXB* online.

Supplementary Table S1. Primers used in qRT-PCR.

Supplementary Table S2. Photosynthetic parameters measured by gas exchange in tomato *GAUT4*-silenced lines.

Supplementary Table S3. Metabolite relative content in *GAUT4*-silenced lines.

Supplementary Fig. S1. Heritability of the silenced phenotype.

Supplementary Fig. S2. Leaf structural analyses of *GAUT4*-silenced plants.

Acknowledgements

F.G., L.B., B.S.L., A.P.S., and J.A. were recipients of FAPESP fellowships. F.C. is a member of CONICET. M.R. and M.S.B. hold fellowships from CNPq. This work was partially supported by grants from FAPESP (Brazil), CNPq (Brazil), USP (Brazil), Instituto Nacional de Ciência e Tecnologia do Bioetanol (Brazil), Max Planck Society (Germany), INTA (Argentina), ANPCyT (Argentina), and CONICET (Argentina), and under the auspices of the EU SOL Integrated Project FOOD-CT-2006-016214.

References

Alim K, Hamant O, Boudaoud A. 2012. Regulatory role of cell division rules on tissue growth heterogeneity. *Frontiers in Plant Science* **3,** 174.

Almeida J, Quadrana L, Asís R, *et al.* 2011. Genetic dissection of vitamin E biosynthesis in tomato. *Journal of Experimental Botany* **62,** 3781–3798.

Altschul SF, Gish W, Miller W, Myers EW, Lipman DJ. 1990. Basic local alignment search tool. *Journal of Molecular Biology* **215,** 403–410.

Arsovski AA, Popma TM, Haughn GW, Carpita NC, McCann MC, Western TL. 2009. AtBXL1 encodes a bifunctional α-D-xylosidase/α-L-arabinofuranosidase required for pectic arabinan modification in *Arabidopsis* mucilage secretory cells. *Plant Physiology* **150,** 1219–1234.

Atmodjo MA, Sakuragi Y, Zhu X, Burrell AJ, Mohanty SS, Atwood JA. 2011. Galacturonosyltransferase (GAUT)1 and GAUT7 are the core of a plant cell wall pectin biosynthetic homogalacturon an:galacturonosyltransferase complex. *Proceedings of the National Academy of Sciences, USA* **50,** 20225–20230.

Bannai H, Tamada Y, Maruyama O, Nakai K, Miyano S. 2002. Extensive feature detection of N-terminal protein sorting signals. *Bioinformatics* **18,** 298–305.

Barrett DM, Garcia E, Wayne JE. 1998. Textural modification of processing tomatoes. *Critical Reviews in Food Science and Nutrition* **38,** 173–258.

Bermúdez L, Urias U, Milstein D, Kamenetzky L, Asis R, Fernie AR, Van Sluys MA, Carrari F, Rossi M. 2008. A candidate gene survey of quantitative trait loci affecting chemical composition in tomato fruit. *Journal of Experimental Botany* **59,** 2875–2890.

Blanc G, Wolfe KH. 2004. Functional divergence of duplicated genes formed by polyploidy during *Arabidopsis* evolution. *Plant Cell* **16,** 1679–1691.

Bombarely A, Menda N, Tecle IY, Buels RM, Strickler S, Fischer-York T, Pujar A, Leto J, Gosselin J, Mueller LA. 2011. The Sol Genomics Network (solgenomics.net): growing tomatoes using Perl. *Nucleic Acids Research* **39,** D1149–D1155.

Bouton S, Leboeuf E, Mouille G, Leydecker MT, Talbotec J, Granier F, Lahaye M, Höfte H, Truong HN. 2002. *QUASIMODO1* encodes a putative membrane-bound glycosyltransferase required for normal pectin synthesis and cell adhesion in *Arabidopsis*. *Plant Cell* **14,** 2577–2590.

Brummell D, Harpster M, Civello P, Palys J, Bennett A, Dunsmuir P. 1999a. Modification of expansin protein abundance in tomato fruit alters softening and cell wall polymer metabolism during ripening. *Plant Cell* **11,** 2203–2216.

Brummell DA, Bird CR, Schuch W, Bennett AB. 1997. An endo-1,4-β-glucanase expressed at high levels in rapidly expanding tissues. *Plant Molecular Biology* **33,** 87–95.

Brummell DA, Hall BD, Bennett AB. 1999b. Antisense suppression of tomato endo-1,4-β-glucanase Cel2 mRNA accumulation increases the force required to break fruit abscission zones but does not affect fruit softening. *Plant Molecular Biology* **40,** 615–622.

Caffall KH, Mohnen D. 2009. The structure, function, and biosynthesis of plant cell wall pectic polysaccharides. *Carbohydrate Research* **344,** 1879–1900.

Caffall KH, Pattathil S, Phillips SE, Hahn MG, Mohnen D. 2009. *Arabidopsis thaliana* T-DNA mutants implicate *GAUT* genes in the biosynthesis of pectin and xylan in cell walls and seed testa. *Molecular Plant* **2,** 1000–1014.

Cantarel BL, Coutinho PM, Rancurel C, Bernard T, Lombard V, Henrissat B. 2009. The Carbohydrate-Active EnZymes database (CAZy): an expert resource for glycogenomics. *Nucleic Acids Research* **37,** D233–D238.

Chaïb J, Lecomte L, Buret M, Causse M. 2006. Stability over genetic backgrounds, generations and years of quantitative trait locus (QTLs) for organoleptic quality in tomato. *Theoretical and Applied Genetics* **112,** 934–944.

Chapman NH, Bonnet J, Grivet L, *et al.* 2012. High-resolution mapping of a fruit firmness-related quantitative trait locus in tomato reveals epistatic interactions associated with a complex combinatorial locus. *Plant Physiology* **159,** 1644–1657.

Chou KC, Shen HB. 2010. Plant-mPLoc: a top-down strategy to augment the power for predicting plant protein subcellular localization. *PLoS ONE* **5,** e11335.

Corpet T. 1988. Multiple sequence alignment with hierarchical clustering. *Nucleic Acids Research* **16,** 10881–10890.

de Souza AP, Arundale RA, Dohleman FG, Long SP, Buckeridge M. 2013. Will the exceptional productivity of *Miscanthus×giganteus* increase further under rising atmospheric CO_2? *Agricultural and Forest Meteorology* 171–172, 82–92.

Di Rienzo JA. 2009. Statistical software for the analysis of experiments of functional genomics. RDNDA, Argentina. http://sites.google.com/site/fgStatistics/

Di Rienzo JA, Casanoves F, Balzarini MG, Gonzalez L, Tablada M, Robledo CW. 2011. InfoStat versión 2011. Grupo InfoStat, FCA, Universidad Nacional de Córdoba, Argentina. http://www.infostat.com.ar.

Emanuelsson O, Brunak S, von Heijne G, Nielsen H. 2007. Locating proteins in the cell using TargetP, SignalP, and related tools. *Nature Protocols* **2,** 953–971.

Fei Z, Joung JG, Tang X, Zheng Y, Huang M, Lee JM, McQuinn R, Tieman DM, Alba R, Klee HJ, Giovannoni JJ. 2011. Tomato Functional Genomics Database: a comprehensive resource and analysis package for tomato functional genomics. *Nucleic Acids Research* **39,** 1156–1163.

Filisetti-Cozzi TMCC, Carpita NC. 1991. Measurement of uronic acids without interference from neutral sugars. *Analytical Biochemstry* **197,** 157–162.

Fridman E, Carrari F, Liu Y, Fernie AR, Zamir D. 2004. Zooming in on a quantitative trait for tomato yield using interspecific introgressions. *Science* **305,** 1786–1789.

Gerrits PO. 1991. *The application of glycol methacrylate in histotechnology; some fundamental principles*. Department of Anatomy and Embryology, State University Groningen, Groningen, The Netherlands.

Giovannoni JJ, DellaPenna D, Bennett AB, Fischer RL. 1989. Expression of a chimeric polygalacturonase gene in transgenic rin (ripening inhibitor) tomato fruit results in polyuronide degradation but not fruit softening. *Plant Cell* **1,** 53–63.

Hackel A, Schauer N, Carrari F, Fernie AR, Grimm B, Kühn C. 2006. Sucrose transporter LeSUT1 and LeSUT2 inhibition affects tomato fruit development in different ways. *The Plant Journal* **45,** 180–192.

Harholt J, Suttangkakul A, Vibe Scheller H. 2010. Biosynthesis of pectin. *Plant Physiology* **153,** 384–395.

Harker FR, Redgwell RJ, Hallett IC, Murray SH, Carter G. 1997. Texture of fresh fruit. *Horticultural Reviews* **20,** 121–224.

Hoeglund A, Doennes P, Blum T, Adolph HW, Kohlbacher O. 2006. MultiLoc: prediction of protein subcellular localization using N-terminal targeting sequences, sequence motifs, and amino acid composition. *Bioinformatics* **22,** 1158–1165.

Houben K, Jolie RP, Fraeye I, Van Loey AM, Hendrickx ME. 2011. Comparative study of the cell wall composition of broccoli, carrot, and tomato: structural characterization of the extractable pectins and hemicelluloses. *Carbohydrate Research* **346,** 1105–1111.

Jones DT, Taylor WR, Thornton JM. 1992. The rapid generation of mutation data matrices from protein sequences. *Computational Applied Biosciences* **8,** 275–282.

Karimi M, Inzé D, Depicker A. 2002. GATEWAY vectors for *Agrobacterium*-mediated plant transformation. *Trends in Plant Science* **7,** 193–195.

Kong Y, Zhou G, Yin Y, Xu Y, Pattathil S, Hahn MG. 2011. Molecular analysis of a family of *Arabidopsis* genes related to galacturonosyltransferases. *Plant Physiology* **155,** 1791–1805.

Kopka J, Schauer N, Krueger S, *et al.* 2005. GMD@CSB.DB: the GolmMetabolome Database. *Bioinformatics* **21,** 1635–1638.

Lahaye M, Devaux MF, Poole M, Seymour GB, Causse M. 2013. Pericarp tissue microstructure and cell wall polysaccharide chemistry are differently affected in lines of tomato with contrasted firmness. *Postharvest Biology and Technology* **76,** 83–90.

Lahaye M, Quemener B, Causse M, Seymour GB. 2012. Hemicellulose fine structure is affected differently during ripening of tomato lines with contrasted texture. *International Journal of Biological Macromolecules* **51,** 462–470.

Leboeuf E, Guillon F, Thoiron S, Lahaye M. 2005. Biochemical and immunohistochemical analysis of pectic polysaccharides in the cell walls of *Arabidopsis* mutant QUASIMODO 1 suspension-cultured cells: implications for cell adhesion. *Journal of Experimental Botany* **56,** 3171–3182.

Lillie RD. 1965. *Histopathologic technic and practical histochemistry*, 3rd edn. New York: McGraw-Hill.

Lisec J, Schauer N, Kopka J, Willmitzer L, Fernie AR. 2006. Gas chromatography mass spectrometry-based metabolite profiling in plants. *Nature Protocols* **1,** 387–396.

Lunn D, Phan TD, Tucker GA, Lycett GW. 2013. Cell wall composition of tomato fruit changes during development and inhibition of vesicle trafficking is associated with reduced pectin levels and reduced softening. *Plant Physiology and Biochemistry* **66,** 91–97.

Maxwell K, Johnson GN. 2000. Chlorophyll fluorescence—a practical guide. *Journal of Experimental Botany* **51,** 659–668.

Mohnen D. 2008. Pectin structure and biosynthesis. *Current Opinion in Plant Biology* **11,** 266–277.

Nelson BK, Cai X, Nebenführ A. (2007). A multicolored set of *in vivo* organelle markers for co-localization studies in *Arabidopsis* and other plants. *The Plant Journal* **51,** 1126–1136.

Nguyen-Quoc B, Foyer CH. 2001. A role for 'futile cycles' involving invertase and sucrose synthase in sucrose metabolism of tomato fruit. *Journal of Experimental Botany* **52,** 881–889.

Nunes-Nesi A, Carrari F, Lytovchenko A, Smith AMO, Loureiro ME, Ratcliffe RG, Sweetlove LJ, Fernie AR. 2005. Enhanced photosynthetic performance and growth as a consequence of

decreasing mitochondrial malate dehydrogenase activity in transgenic tomato plants. *Plant Physiology* **137,** 611–622.

O'Brien TP, Feder N, McCully ME. 1964. Polychromatic staining of plant cell walls by toluidine blue O. *Protoplasma* **59,** 368–373.

Oms-Oliu G, Hertog MLATM, Van de Poel B, Ampofo-Asiama J, Geeraerd AH, Nicolaï BM. 2011. Metabolic characterization of tomato fruit during preharvest development, ripening, and postharvest shelf-life. *Postharvest Biology and Technology* **62,** 7–16.

Oomen RJFJ, Doeswijk-Voragen CHL, Bush MS, *et al.* 2002. *In muro* fragmentation of the rhamnogalacturonan I backbone in potato (*Solanum tuberosum* L.) results in a reduction and altered location of the galactan and arabinan side-chains and abnormal periderm development. *The Plant Journal* **30,** 403–413.

Orfila C, Sørensen SO, Harholt J, Geshi N, Crombie H, Truong HN, Reid JSG, Knox JP, Scheller HV. 2005. QUASIMODO1 is expressed in vascular tissue of *Arabidopsis thaliana* inflorescence stems, and affects homogalacturonan and xylan biosynthesis. *Planta* **222,** 613–622.

Osorio S, Alba R, Nikoloski Z, Kochevenko A, Fernie AR, Giovannoni JJ. 2012. Integrative comparative analyses of transcript and metabolite profiles from pepper and tomato ripening and development stages uncovers species-specific patterns of network regulatory behavior. *Plant Physiology* **159,** 1713–1729.

Patrick JW, Offler CE. 1996. Post-sieve element transport of photoassimilates in sink regions. *Journal of Experimental Botany* **47,** 1165–1177.

Peña M J, Zhong R, Zhou G, Richardson EA, O'Neill MA, Darvill AG, York WS, Ye Z. 2007. *Arabidopsis irregular xylem8* and *irregular xylem9*: implications for the complexity of glucuronoxylan biosynthesis. *Plant Cell* **19,** 549–563.

Persson S, Caffall KH, Freshour G, Hilley MT, Bauer S, Poindexter P, Hahn MG, Mohnen D, Somerville C. 2007. The *Arabidopsis irregular xylem8* mutant is deficient in glucuronoxylan and homogalacturonan, which are essential for secondary cell wall integrity. *Plant Cell* **19,** 237–255.

Rasband WS. 1997–2012. ImageJ. US National Institutes of Health, Bethesda, Maryland, USA. http://imagej.nih.gov/ij/.

Reiter WD. 2008. Biochemical genetics of nucleotide sugar interconversion reactions. *Current Opinion in Plant Biology* **11,** 236–243.

Ridley BL, Neill MAO, Mohnen D. 2001. Pectins: structure, biosynthesis, and oligogalacturonide-related signaling. *Phytochemistry* **57,** 929–967.

Roessner U, Willmitzer L, Fernie AR. 2001. High-resolution metabolic phenotyping of genetically and environmentally diverse potato tuber systems. Identification of phenocopies. *Plant Physiology* **127,** 749–764.

Ruijter JM, Ramakers C, Hoogaars WMH, Karlen Y, Bakker O, van den Hoff MJB, Moorman AFM. 2009. Amplification efficiency: linking baseline and bias in the analysis of quantitative PCR data. *Nucleic Acids Research* **37,** e45.

Saeed AI, Sharov V, White J, *et al.* 2003. TM4: a free, open-source system for microarray data management and analysis. *Biotechniques* **34,** 374–378.

Saeman JF, Bulb JL, Harris EE. 1945. Quantitative saccharification of wood and cellulose. *Industrial and Engineering Chemistry* **17,** 35–37.

Saladié M, Matas AJ, Isaacson T, *et al.* 2007. A reevaluation of the key factors that influence tomato fruit softening and integrity. *Plant Physiology* **144,** 1012–1028.

Schauer N, Semel Y, Roessner U, *et al.* 2006. Comprehensive metabolic profiling and phenotyping of interspecific introgression lines for tomato improvement. *Nature Biotechnology* **24,** 447–454.

Schauer N, Steinhauser D, Strelkov S, *et al.* 2005. GC-MS libraries for the rapid identification of metabolites in complex biological samples. *Federation of European Biochemical Societies Letters* **579,** 1332–1337.

Shackel KA, Greve C, Labavitch JM, Ahmadi H. 1991. Cell turgor changes associated with ripening in tomato pericarp tissue. *Plant Physiology* **97,** 814–816.

Shatkay H, Höglund A, Brady S, Blum T, Dönnes P, Kohlbacher O. 2007. SherLoc: high-accuracy prediction of protein subcellular localization by integrating text and protein sequence data. *Bioinformatics* **23,** 1410–1417.

Sienkiewicz-Porzucek A, Sulpice R, Osorio S, Krahnert I, Leisse A, Urbanczyk-Wochniak E, Hodges M, Fernie AR, Nunes-Nesi A. 2010. Mild reductions in mitochondrial NAD-dependent isocitrate dehydrogenase activity result in altered nitrate assimilation and pigmentation but do not impact growth. *Molecular Plant* **3,** 156–173.

Sila DN, Buggenhout SV, Duvetter T, Fraeye I, Roeck AD, Loey AV, Hendrickx M. 2009. Pectins in processed fruits and vegetables: part II. Structure–function relationships. *Comprehensive Reviews in Food Science and Food Safety* **8,** 86–104.

Smith DL, Abbott JA, Gross KC. 2002. Down-regulation of tomato β-galactosidase 4 results in decreased fruit softening. *Plant Physiology* **129,** 1755–1762.

Song C, Guo J, Sun W, Wang Y. 2012. Whole genome duplication of intra-and inter-chromosomes in the tomato genome. *Journal of Genetics and Genomics* **39,** 361–368.

Sterling JD, Atmodjo MA, Inwood SE, Kumar Kolli VS, Quigley HF, Hahn MG, Mohnen D. 2006. Functional identification of an *Arabidopsis* pectin biosynthetic homogalacturonan galacturonosyltransferase. *Proceedings of the National Academy of Sciences, USA* **103,** 5236–5241.

Szymanski DB, Cosgrove DJ. 2009. Dynamic coordination of cytoskeletal and cell wall systems during plant cell morphogenesis. *Current Biology* **19,** 800–811.

Tamura K, Peterson D, Peterson N, Stecher G, Nei M, Kumar S. 2011. MEGA5: molecular evolutionary genetics analysis using maximum likelihood, evolutionary distance, and maximum parsimony methods. *Molecular Biology and Evolution* **28,** 2731–2739.

The Tomato Genome Consortium. 2012. The tomato genome sequence provides insights into fleshy fruit evolution. *Nature* **485,** 635–641.

Thompson JD, Higgins DG, Gibson TJ. 1997. The CLUSTAL_X windows interface: flexible strategies for multiple sequence alignment aided by quality analysis tools. *Nucleic Acids Research* **25,** 4876–4882.

Tieman DM, Harriman RW, Ramamohan G, Handa AK. 1992. An antisense pectin methylesterase gene alters pectin chemistry and

soluble solids in tomato fruit. *Plant Cell* **4,** 667–679.

Unda F, Canam T, Preston L, Mansfield SD. 2012. Isolation and characterization of galactinol synthases from hybrid poplar. *Journal of Experimental Botany* **63,** 2059–2069.

Vincken JP, Schols HA, Oomen RJFJ, McCann MC, Ulvskov P, Voragen AGJ, Visser RGF. 2003. If homogalacturonan were a side chain of rhamnogalacturonan I. Implications for cell wall architecture. *Plant Physiology* **132,** 1781–1789.

Voorrips RE. 2002. MapChart: software for the graphical presentation of linkage maps and QTLs. *Journal of Heredity* **93,** 77–78.

Wormit A, Butt SM, Chairam I, *et al.* 2012. Osmosensitive changes of carbohydrate metabolism in response to cellulose biosynthesis inhibition. *Plant Physiology* **159,** 105–117.

Yin Y, Chen H, Hahn MG, Mohnen D, Xu Y. 2010. Evolution and function of the plant cell wall synthesis-related glycosyltransferase family 8. *Plant Physiology* **153,** 1729–1746.

Zhou T, Zhang R, Guo S. 2011. Molecular cloning and characterization of *GhGolS1*, a novel gene encoding galactinol synthase from cotton (*Gossypium hirsutum*). *Plant Molecular Biology Report* **30,** 699–709.